SECTION 4
ANALYSIS OF SPECIAL STRUCTURES

Louis F. Geschwindner*, P.E.
Professor of Architectural Engineering,
The Pennsylvania State University,
University Park, Pennsylvania

The general structural theory presented in Sec. 3 can be used to analyze practically all types of structural steel framing. For some frequently used complex framing, however, a specific adaptation of the general theory often expedites the analysis. In some cases, for example, formulas for reactions can be derived from the general theory. Then the general theory is no longer needed for an analysis. In some other cases, where use of the general theory is required, specific methods can be developed to simplify analysis.

This section presents some of the more important specific formulas and methods for complex framing. Usually, several alternative methods are available, but space does not permit their inclusion. The methods given in the following were chosen for their general utility when analysis will not be carried out with a computer.

4.1 THREE-HINGED ARCHES

An **arch** is a beam curved in the plane of the loads to a radius that is very large relative to the depth of section. Loads induce both bending and direct compressive stress. Reactions have horizontal components, though all loads are vertical. Deflections, in general, have horizontal as well as vertical components. At supports, the horizontal components of the reactions must be resisted. For the purpose, tie rods, abutments, or buttresses may be used. With a series of arches, however, the reactions of an interior arch may be used to counteract those of adjoining arches.

A three-hinged arch is constructed by inserting a hinge at each support and at an internal point, usually the crown, or high point (Fig. 4.1). This construction is statically determinate. There are four unknowns—two horizontal and two vertical components of the reactions—but four equations based on the laws of equilibrium are available.

*Revised Sec. 4, originally authored by Frederick S. Merritt, Consulting Engineer, West Palm Beach, Florida.

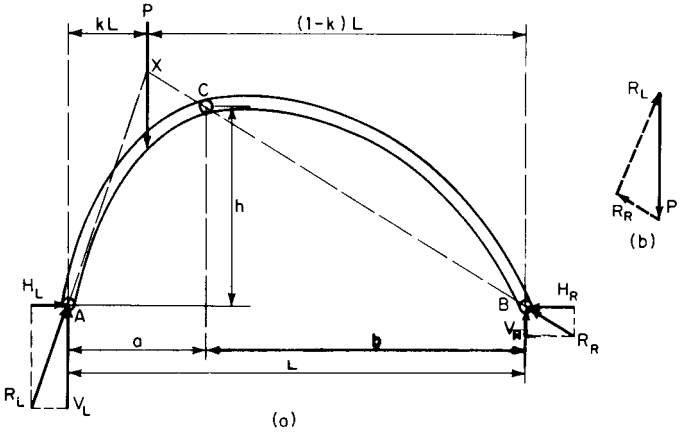

FIGURE 4.1 Three-hinged arch. (*a*) Determination of line of action of reactions. (*b*) Determination of reactions.

1. The sum of the horizontal forces acting on the arch must be zero. This relates the horizontal components of the reactions:

$$H_L = H_R = H \tag{4.1}$$

2. The sum of the moments about the left support must be zero. For the arch in Fig. 4.1, this determines the vertical component of the reaction at the right support:

$$V_R = Pk \tag{4.2}$$

where P = load at distance kL from left support
L = span

3. The sum of the moments about the right support must be zero. This gives the vertical component of the reaction at the left support:

$$V_L = P(1 - k) \tag{4.3}$$

4. The bending moment at the crown hinge must be zero. (The sum of the moments about the crown hinge also is zero but does not provide an independent equation for determination of the reactions.) For the right half of the arch in Fig. 4.1, $Hh - V_R b = 0$, from which

$$H = \frac{V_R b}{h} = \frac{Pkb}{h} \tag{4.4}$$

The influence line for H for this portion of the arch thus is a straight line, varying from zero for a unit load over the support to a maximum of ab/Lh for a unit load at C.

Reactions of three-hinge arches also can be determined graphically by taking advantage of the fact that the bending moment at the crown hinge is zero. This requires that the line of action of reaction R_R at the right support pass through C. This line intersects the line of action of load P at X (Fig. 4.1). Because P and the two reactions are in equilibrium, the line of action of reaction R_L at the left support also must pass through X. As indicated in Fig. 4.1*b*, the magnitudes of the reactions can be found from a force triangle comprising P and the lines of action of the reactions.

For additional concentrated loads, the results may be superimposed to obtain the final horizontal and vertical reactions. Since the three hinged arch is determinate, the same four

equations of equilibrium can be applied and the corresponding reactions determined for any other loading condition. It should also be noted that what is important is not the shape of the arch, but the location of the internal hinge in relation to the support hinges.

After the reactions have been determined, the stresses at any section of the arch can be found by application of the equilibrium laws (Art. 4.4).

(T. Y. Lin and S.D. Stotesbury, *Structural Concepts and Systems for Architects and Engineers,* 2d Ed., Van Nostrand Reinhold Company, New York.)

4.2 TWO-HINGED ARCHES

A two-hinged arch has hinges only at the supports (Fig. 4.2*a*). Such an arch is statically indeterminate. Determination of the horizontal and vertical components of each reaction requires four equations, whereas the laws of equilibrium supply only three (Art. 4.1).

Another equation can be written from knowledge of the elastic behavior of the arch. One procedure is to assume that one of the supports is on rollers. The arch then becomes statically determinate. Reactions V_L and V_R and horizontal movement of the support δx can be computed for this condition with the laws of equilibrium (Fig. 4.2*b*). Next, with the support still on rollers, the horizontal force H required to return the movable support to its original position can be calculated (Fig. 4.2*c*). Finally, the reactions of the two-hinged arch of Fig. 4.2*a* are obtained by adding the first set of reactions to the second (Fig. 4.2*d*).

The structural theory of Sec. 3 can be used to derive a formula for the horizontal component H of the reactions. For example, for the arch of Fig. 4.2*a*, δx is the horizontal movement of the support due to loads on the arch. Application of virtual work gives

$$\delta x = \int_A^B \frac{My\, ds}{EI} - \int_A^B \frac{N\, dx}{AE} \tag{4.5}$$

where M = bending moment at any section due to loads on the arch
y = vertical ordinate of section measured from immovable hinge

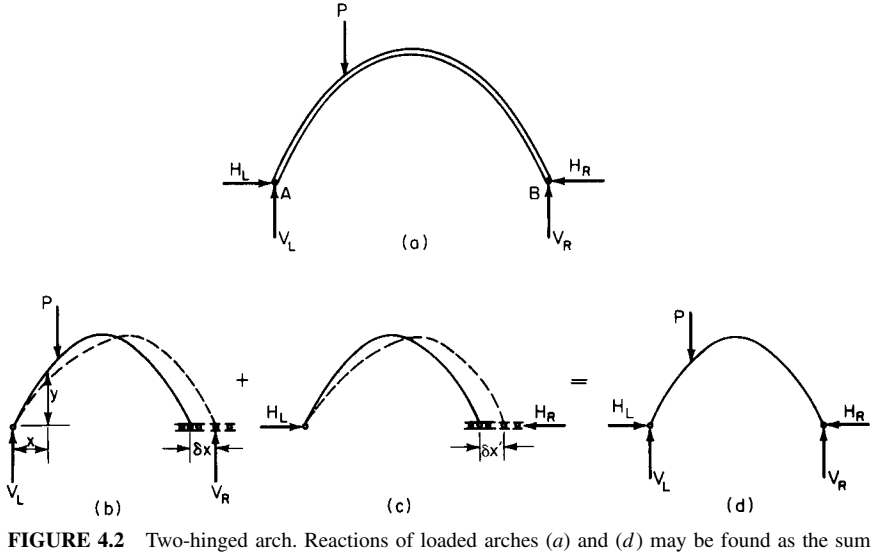

FIGURE 4.2 Two-hinged arch. Reactions of loaded arches (*a*) and (*d*) may be found as the sum of reactions in (*b*) and (*c*) with one support movable horizontally.

I = moment of inertia of arch cross section
A = cross-sectional area of arch at the section
E = modulus of elasticity
ds = differential length along arch axis
dx = differential length along the horizontal
N = normal thrust on the section due to loads

Unless the thrust is very large, the second term on the right of Eq. (4.5) can be ignored.

Let $\delta x'$ be the horizontal movement of the support due to a unit horizontal force applied to the hinge. Application of virtual work gives

$$\delta x' = -\int_A^B \frac{y^2\, ds}{EI} - \int_A^B \frac{\cos^2 \alpha\, dx}{AE} \tag{4.6}$$

where α is the angle the tangent to axis at the section makes with horizontal. Neither this equation nor Eq. (4.5) includes the effect of shear deformation and curvature. These usually are negligible.

In most cases, integration is impracticable. The integrals generally must be evaluated by approximate methods. The arch axis is divided into a convenient number of elements of length Δs, and the functions under the integral sign are evaluated for each element. The sum of the results is approximately equal to the integral.

For the arch of Fig. 4.2,

$$\delta x + H\, \delta x' = 0 \tag{4.7}$$

When a tie rod is used to take the thrust, the right-hand side of the equation is not zero but the elongation of the rod HL/A_sE, where L is the length of the rod and A_s its cross-sectional area. The effect of an increase in temperature Δt can be accounted for by adding to the left-hand side of the equation $c\Delta tL$, where L is the arch span and c the coefficient of expansion.

For the usual two-hinged arch, solution of Eq. (4.7) yields

$$H = -\frac{\delta x}{\delta x'} = \frac{\sum_A^B (My\ \Delta s/EI) - \sum_A^B N \cos\alpha\ \Delta s/AE}{\sum_A^B (y^2\ \Delta s/EI) + \sum_A^B (\cos^2 \alpha\ \Delta s/AE)} \tag{4.8}$$

After the reactions have been determined, the stresses at any section of the arch can be found by application of the equilibrium laws (Art. 4.4).

Circular Two-Hinged Arch Example. A circular two-hinged arch of 175-ft radius with a rise of 29 ft must support a 10-kip load at the crown. The modulus of elasticity E is constant, as is I/A, which is taken as 40.0. The arch is divided into 12 equal segments, 6 on each symmetrical half. The elements of Eq. (4.8) are given in Table 4.1 for each arch half.

Since the increment along the arch is as a constant, it will factor out of Eq. 4.8. In addition, the modulus of elasticity will cancel when factored. Thus, with A and I as constants, Eq. 4.8 may be simplified to

$$H = \frac{\sum_B^A My - \frac{I}{A}\sum_B^A N \cos\ \alpha}{\sum_B^A y^2 + \frac{I}{A}\sum_B^A \cos^2\ \alpha} \tag{4.8a}$$

From Eq. (4.8) and with the values in Table 4.1 for one-half the arch, the horizontal reaction may be determined. The flexural contribution yields

TABLE 4.1 Example of Two-Hinged Arch Analysis

α radians	My, kip-ft^2	y^2, ft^2	$N \cos \alpha$ kips	$\cos^2 \alpha$
0.0487	12,665	829.0	0.24	1.00
0.1462	9,634	736.2	0.72	0.98
0.2436	6,469	568.0	1.17	0.94
0.3411	3,591	358.0	1.58	0.89
0.4385	1,381	154.8	1.92	0.82
0.5360	159	19.9	2.20	0.74
TOTAL	33,899	2,665.9	7.83	5.37

$$H = \frac{2.0(33899)}{2.0(2665.9)} = 12.71 \text{ kips}$$

Addition of the axial contribution yields

$$H = \frac{2.0[33899 - 40.0(7.83)]}{2.0[2665.9 + 40.0(5.37)]} = 11.66 \text{ kips}$$

It may be convenient to ignore the contribution of the thrust in the arch under actual loads. If this is the case, $H = 11.77$ kips.

(F. Arbabi, *Structural Analysis and Behavior,* McGraw-Hill Inc. New York.)

4.3 FIXED ARCHES

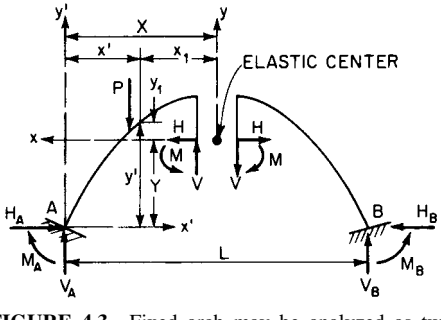

FIGURE 4.3 Fixed arch may be analyzed as two cantilevers.

In a **fixed arch,** translation and rotation are prevented at the supports (Fig. 4.3). Such an arch is statically indeterminate. With each reaction comprising a horizontal and vertical component and a moment (Art. 4.1), there are a total of six reaction components to be determined. Equilibrium laws provide only three equations. Three more equations must be obtained from a knowledge of the elastic behavior of the arch.

One procedure is to consider the arch cut at the crown. Each half of the arch then becomes a cantilever. Loads along each cantilever cause the free ends to deflect and rotate. To permit the cantilevers to be joined at the free ends to restore the original fixed arch, forces must be applied at the free ends to equalize deflections and rotations. These conditions provide three equations.

Solution of the equations, however, can be simplified considerably if the center of coordinates is shifted to the elastic center of the arch and the coordinate axes are properly oriented. If the unknown forces and moments V, H, and M are determined at the elastic center (Fig. 4.3), each equation will contain only one unknown. When the unknowns at the elastic center have been determined, the shears, thrusts, and moments at any points on the arch can be found from the laws of equilibrium.

Determination of the location of the elastic center of an arch is equivalent to finding the center of gravity of an area. Instead of an increment of area dA, however, an increment of length ds multiplied by a width $1/EI$ must be used, where E is the modulus of elasticity and I the moment of inertia of the arch cross section.

In most cases, integration is impracticable. An approximate method is usually used, such as the one described in Art. 4.2.

Assume the origin of coordinates to be temporarily at A, the left support of the arch. Let x' be the horizontal distance from A to a point on the arch and y' the vertical distance from A to the point. Then the coordinates of the elastic center are

$$X = \frac{\sum_A^B (x'\ \Delta s/EI)}{\sum_A^B (\Delta s/EI)} \qquad Y = \frac{\sum_A^B (y'\ \Delta s/EI)}{\sum_A^B (\Delta s/EI)} \tag{4.9}$$

If the arch is symmetrical about the crown, the elastic center lies on a normal to the tangent at the crown. In this case, there is a savings in calculation by taking the origin of the temporary coordinate system at the crown and measuring coordinates parallel to the tangent and the normal. Furthermore, Y, the distance of the elastic center from the crown, can be determined from Eq. (4.9) with y' measured from the crown and the summations limited to the half arch between crown and either support. For a symmetrical arch also, the final coordinates should be chosen parallel to the tangent and normal to the crown.

For an unsymmetrical arch, the final coordinate system generally will not be parallel to the initial coordinate system. If the origin of the initial system is translated to the elastic center, to provide new temporary coordinates $x_1 = x' - X$ and $y_1 = y' - Y$, the final coordinate axes should be chosen so that the x axis makes an angle α, measured clockwise, with the x_1 axis such that

$$\tan 2\alpha = \frac{2\sum_A^B (x_1 y_1\ \Delta s/EI)}{\sum_A^B (x_1^2\ \Delta s/EI) - \sum_A^B (y_1^2\ \Delta s/EI)} \tag{4.10}$$

The unknown forces H and V at the elastic center should be taken parallel, respectively, to the final x and y axes.

The free end of each cantilever is assumed connected to the elastic center with a rigid arm. Forces H, V, and M act against this arm, to equalize the deflections produced at the elastic center by loads on each half of the arch. For a coordinate system with origin at the elastic center and axes oriented to satisfy Eq. (4.10), application of virtual work to determine deflections and rotations yields

$$H = \frac{\sum_A^B (M'y\ \Delta s/EI)}{\sum_A^B (y^2\ \Delta s/EI)}$$

$$V = \frac{\sum_A^B (M'x\ \Delta s/EI)}{\sum_A^B (x^2\ \Delta s/EI)} \tag{4.11}$$

$$M = \frac{\sum_{A}^{B} (M' \, \Delta s/EI)}{\sum_{A}^{B} (\Delta s/EI)}$$

where M' is the average bending moment on each element of length Δs due to loads. To account for the effect of an increase in temperature t, add $EctL$ to the numerator of H, where c is the coefficient of expansion and L the distance between abutments. Equations (4.11) may be similarly modified to include deformations due to secondary stresses.

With H, V, and M known, the reactions at the supports can be determined by application of the equilibrium laws. In the same way, the stresses at any section of the arch can be computed (Art. 4.4).

(S. Timoshenko and D. H. Young, *Theory of Structures,* McGraw-Hill, Inc., New York; S. F. Borg and J. J. Gennaro, *Advanced Structural Analysis,* Van Nostrand Reinhold Company, New York; G. L. Rogers and M. L. Causey, *Mechanics of Engineering Structures,* John Wiley & Sons, Inc., New York; J. Michalos, *Theory of Structural Analysis and Design,* The Ronald Press Company, New York.)

4.4 STRESSES IN ARCH RIBS

When the reactions have been determined for an arch (Arts. 4.1 to 4.3), the principal forces acting on any cross section can be found by applying the equilibrium laws. Suppose, for example, the forces H, V, and M acting at the elastic center of a fixed arch have been computed, and the moment M_x, shear S_x, and axial thrust N_x normal to a section at X (Fig. 4.4) are to be determined. H, V, and the load P may be resolved into components parallel to the thrust and shear, as indicated in Fig. 4.4. Then, equating the sum of the forces in each direction to zero gives

$$\begin{aligned} N_x &= V \sin \theta_x + H \cos \theta_x + P \sin(\theta_x - \theta) \\ S_x &= V \cos \theta_x - H \sin \theta_x + P \cos(\theta_x - \theta) \end{aligned} \tag{4.12}$$

Equating moments about X to zero yields

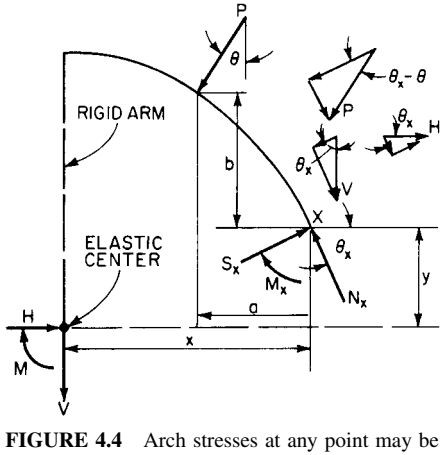

FIGURE 4.4 Arch stresses at any point may be determined from forces at the elastic center.

$$M_x = Vx + Hy - M + Pa \cos \theta + Pb \sin \theta \tag{4.13}$$

For structural steel members, the shearing force on a section usually is assumed to be carried only by the web. In built-up members, the shear determines the size and spacing of fasteners or welds between web and flanges. The full (gross) section of the arch rib generally is assumed to resist the combination of axial thrust and moment.

4.5 PLATE DOMES

A **dome** is a three-dimensional structure generated by translation and rotation or only rotation of an arch rib. Thus a dome may be part of a sphere, ellipsoid, paraboloid, or similar curved surface.

Domes may be thin-shell or framed, or a combination. Thin-shell domes are constructed of sheet metal or plate, braced where necessary for stability, and are capable of transmitting loads in more than two directions to supports. The surface is substantially continuous from crown to supports. Framed domes, in contrast, consist of interconnected structural members lying on the dome surface or with points of intersection lying on the dome surface (Art. 4.6). In combination construction, covering material may be designed to participate with the framework in resisting dome stresses.

Plate domes are highly efficient structurally when shaped, proportioned and supported to transmit loads without bending or twisting. Such domes should satisfy the following conditions:

The plate should not be so thin that deformations would be large compared with the thickness. Shearing stresses normal to the surface should be negligible. Points on a normal to the surface before it is deformed should lie on a straight line after deformation. And this line should be normal to the deformed surface.

Stress analysis usually is based on the membrane theory, which neglects bending and torsion. Despite the neglected stresses, the remaining stresses are in equilibrium, except possibly at boundaries, supports, and discontinuities. At any interior point of a thin-shell dome, the number of equilibrium conditions equals the number of unknowns. Thus, in the membrane theory, a plate dome is statically determinate.

The membrane theory, however, does not hold for certain conditions: concentrated loads normal to the surface and boundary arrangements not compatible with equilibrium or geometric requirements. Equilibrium or geometric incompatibility induces bending and torsion in the plate. These stresses are difficult to compute even for the simplest type of shell and loading, yet they may be considerably larger than the membrane stresses. Consequently, domes preferably should be designed to satisfy membrane theory as closely as possible.

Make necessary changes in dome thickness gradual. Avoid concentrated and abruptly changing loads. Change curvature gradually. Keep discontinuities to a minimum. Provide reactions that are tangent to the dome. Make certain that the reactions at boundaries are equal in magnitude and direction to the shell forces there. Also, at boundaries, ensure, to the extent possible, compatibility of shell deformations with deformations of adjoining members, or at least keep restraints to a minimum. A common procedure is to use as a support a husky ring girder and to thicken the shell gradually in the vicinity of this support. Similarly, where a circular opening is provided at the crown, the opening usually is reinforced with a ring girder, and the plate is made thicker than necessary for resisting membrane stresses.

Dome surfaces usually are generated by rotating a plane curve about a vertical axis, called the **shell axis.** A plane through the axis cuts the surface in a meridian, whereas a plane normal to the axis cuts the surface in a circle, called a **parallel** (Fig. 4.5*a*). For stress analysis, a coordinate system for each point is chosen with the x axis tangent to the meridian, y axis

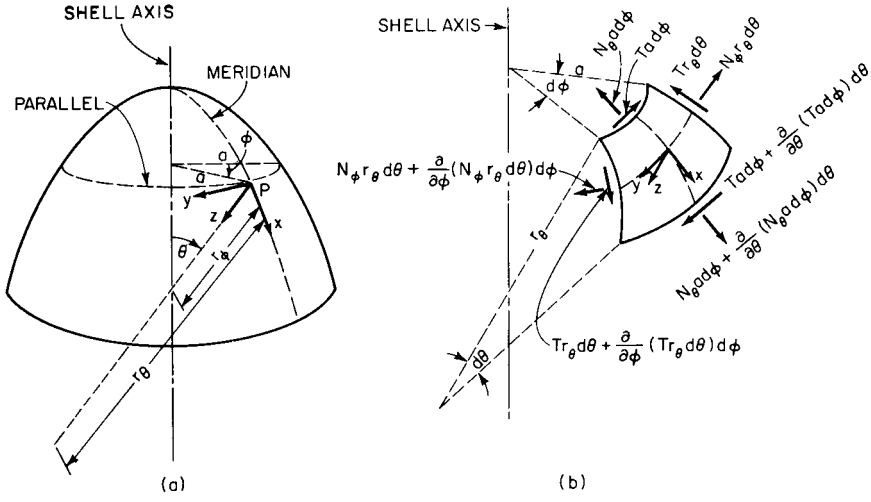

FIGURE 4.5 Thin-shell dome. (*a*) Coordinate system for analysis. (*b*) Forces acting on a small element.

tangent to the parallel, and z axis normal to the surface. The membrane forces at the point are resolved into components in the directions of these axes (Fig. 4.5*b*).

Location of a given point P on the surface is determined by the angle θ between the shell axis and the normal through P and by the angle ϕ between the radius through P of the parallel on which P lies and a fixed reference direction. Let r_θ be the radius of curvature of the meridian. Also, let r_ϕ, the length of the shell normal between P and the shell axis, be the radius of curvature of the normal section at P. Then,

$$r_\phi = \frac{a}{\sin \theta} \tag{4.14}$$

where a is the radius of the parallel through P.

Figure 4.5*b* shows a differential element of the dome surface at P. Normal and shear forces are distributed along each edge. They are assumed to be constant over the thickness of the plate. Thus, at P, the meridional unit force is N_θ, the unit hoop force N_ϕ, and the unit shear force T. They act in the direction of the x or y axis at P. Corresponding unit stresses at P are N_θ/t, N_ϕ/t, and T/t, where t is the plate thickness.

Assume that the loading on the element per unit of area is given by its X, Y, Z components in the direction of the corresponding coordinate axis at P. Then, the equations of equilibrium for a shell of revolution are

$$\begin{aligned}
\frac{\partial}{\partial \theta}(N_\theta r_\phi \sin \theta) + \frac{\partial T}{\partial \phi} r_\theta - N_\phi r_\theta \cos \theta + X r_\theta r_\phi \sin \theta &= 0 \\
\frac{\partial N_\phi}{\partial \phi} r_\theta + \frac{\partial}{\partial \theta}(T r_\phi \sin \theta) + T r_\theta \cos \theta + Y r_\theta r_\phi \sin \theta &= 0 \\
N_\theta r_\phi + N_\phi r_\theta + Z r_\theta r_\phi &= 0
\end{aligned} \tag{4.15}$$

When the loads also are symmetrical about the shell axis, Eqs. (4.15) take a simpler form and are easily solved, to yield

$$N_\theta = -\frac{R}{2\pi a}\sin\theta = -\frac{R}{2\pi r_\phi}\sin^2\theta \tag{4.16}$$

$$N_\phi = \frac{R}{2\pi r_\theta}\sin^2\theta - Zr_\phi \tag{4.17}$$

$$T = 0 \tag{4.18}$$

where R is the resultant of total vertical load above parallel with radius a through point P at which stresses are being computed.

For a spherical shell, $r_\theta = r_\phi = r$. If a vertical load p is uniformly distributed over the horizontal projection of the shell, $R = \pi a^2 p$. Then the unit meridional thrust is

$$N_\theta = -\frac{pr}{2} \tag{4.19}$$

Thus there is a constant meridional compression throughout the shell. The unit hoop force is

$$N_\phi = -\frac{pr}{2}\cos 2\theta \tag{4.20}$$

The hoop forces are compressive in the upper half of the shell, vanish at $\theta = 45°$, and become tensile in the lower half.

If, for a spherical dome, a vertical load w is uniform over the area of the shell, as might be the case for the weight of the shell, then $R = 2\pi r^2(1 - \cos\theta)w$. From Eqs. (4.16) and (4.17), the unit meridional thrust is

$$N_\theta = -\frac{wr}{1 + \cos\theta} \tag{4.21}$$

In this case, the compression along the meridian increases with θ. The unit hoop force is

$$N_\phi = wr\left(\frac{1}{1 + \cos\theta} - \cos\theta\right) \tag{4.22}$$

The hoop forces are compressive in the upper part of the shell, reduce to zero at 51°50′, and become tensile in the lower part.

A ring girder usually is provided along the lower boundary of a dome to resist the tensile hoop forces. Under the membrane theory, however, shell and girder will have different strains. Consequently, bending stresses will be imposed on the shell. Usual practice is to thicken the shell to resist these stresses and provide a transition to the husky girder.

Similarly, when there is an opening around the crown of the dome, the upper edge may be thickened or reinforced with a ring girder to resist the compressive hoop forces. The meridional thrust may be computed from

$$N_\theta = -wr\frac{\cos\theta_0 - \cos\theta}{\sin^2\theta} - P\frac{\sin\theta_0}{\sin^2\theta} \tag{4.23}$$

and the hoop forces from

$$N_\phi = wr\left(\frac{\cos\theta_0 - \cos\theta}{\sin^2\theta} - \cos\theta\right) + P\frac{\sin\theta_0}{\sin^2\theta} \tag{4.24}$$

where $2\theta_0$ = angle of opening
P = vertical load per unit length of compression ring

4.6 RIBBED DOMES

As pointed out in Art. 4.5, domes may be thin-shell, framed, or a combination. One type of framed dome consists basically of arch ribs with axes intersecting at a common point at the crown and with skewbacks, or bases, uniformly spaced along a closed horizontal curve. Often, to avoid the complexity of a joint with numerous intersecting ribs at the crown, the arch ribs are terminated along a compression ring circumscribing the crown. This construction also has the advantage of making it easy to provide a circular opening at the crown should this be desired. Stress analysis is substantially the same whether or not a compression ring is used. In the following, the ribs will be assumed to extend to and be hinged at the crown. The bases also will be assumed hinged. Thrust at the bases may be resisted by abutments or a tension ring.

Despite these simplifying assumptions, such domes are statically indeterminate because of the interaction of the ribs at the crown. Degree of indeterminacy also is affected by deformations of tension and compression rings. In the following analysis, however, these deformations will be considered negligible.

It usually is convenient to choose as unknowns the horizontal component H and vertical component V of the reaction at the bases of each rib. In addition, an unknown force acts at the crown of each rib. Determination of these forces requires solution of a system of equations based on equilibrium conditions and common displacement of all rib crowns. Resistance of the ribs to torsion and bending about the vertical axis is considered negligible in setting up these equations.

As an example of the procedure, equations will be developed for analysis of a spherical dome under unsymmetrical loading. For simplicity, Fig. 4.6 shows only two ribs of such a dome. Each rib has the shape of a circular arc. Rib $1C1'$ is subjected to a load with horizontal component P_H and vertical component P_V. Coordinates of the load relative to point 1 are (x_P, y_P). Rib $2C2'$ intersects rib $1C1'$ at the crown at an angle $\alpha_r \leq \pi/2$. A typical rib rCr' intersects rib $1C1'$ at the crown at an angle $\alpha_r \leq \pi/2$. The dome contains n identical ribs.

A general coordinate system is chosen with origin at the center of the sphere which has radius R. The base of the dome is assigned a radius r. Then, from the geometry of the sphere,

$$\cos \phi_1 = \frac{r}{R} \tag{4.25}$$

For any point (x, y),

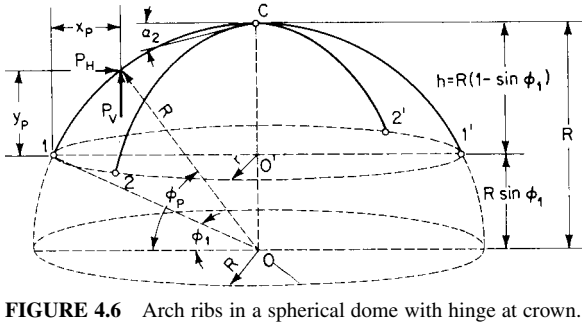

FIGURE 4.6 Arch ribs in a spherical dome with hinge at crown.

$$x = R(\cos \phi_1 - \cos \phi) \tag{4.26}$$

$$y = R(\sin \phi - \sin \phi_1) \tag{4.27}$$

And the height of the crown is

$$h = R(1 - \sin \phi_1) \tag{4.28}$$

where ϕ_1 = angle radius vector to point 1 makes with horizontal
ϕ = angle radius vector to point (x, y) makes with horizontal

Assume temporarily that arch $1C1'$ is disconnected at the crown from all the other ribs. Apply a unit downward vertical load at the crown (Fig. 4.7*a*). This produces vertical reactions $V_1 = V_{1'} = \frac{1}{2}$ and horizontal reactions

$$H_1 = -H_{1'} = r/2h = \cos \phi_1/2(1 - \sin \phi_1)$$

Here and in the following discussion upward vertical loads and horizontal loads acting to the right are considered positive. At the crown, downward vertical displacements and horizontal displacements to the right will be considered positive.

For $\phi_1 \leq \phi \leq \pi/2$, the bending moment at any point (x, y) due to the unit vertical load at the crown is

$$m_V = \frac{x}{2} - \frac{ry}{2h} = \frac{r}{2}\left(1 - \frac{\cos \phi}{\cos \phi_1} - \frac{\sin \phi - \sin \phi_1}{1 - \sin \phi_1}\right) \tag{4.29}$$

For $\pi/2 \leq \phi \leq \pi$,

$$m_V = \frac{r}{2}\left(1 + \frac{\cos \phi}{\cos \phi_1} - \frac{\sin \phi - \sin \phi_1}{1 - \sin \phi_1}\right) \tag{4.30}$$

By application of virtual work, the downward vertical displacement d_V of the crown produced by the unit vertical load is obtained by dividing the rib into elements of length Δs and computing

$$d_V = \sum_{1}^{1'} \frac{m_V^2 \, \Delta s}{EI} \tag{4.31}$$

where E = modulus of elasticity of steel
I = moment of inertia of cross section about horizontal axis

The summation extends over the length of the rib.

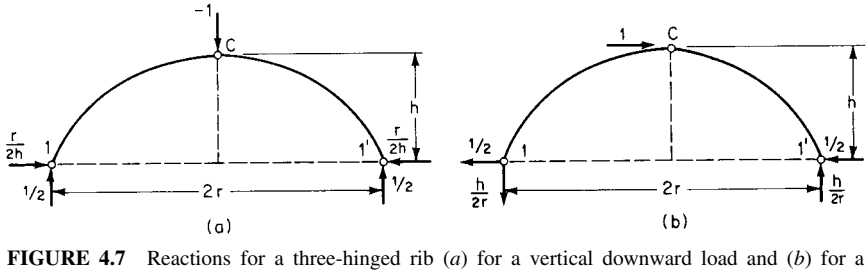

FIGURE 4.7 Reactions for a three-hinged rib (*a*) for a vertical downward load and (*b*) for a horizontal load at the crown.

Next, apply at the crown a unit horizontal load acting to the right (Fig. 4.7*b*). This produces vertical reactions $V_1 = -V_{1'} = -h/2r = -(1 - \sin \phi_1)/2 \cos \phi_1$ and $H_1 = H_{1'} = -\frac{1}{2}$.

For $\phi_1 \le \phi \le \pi/2$, the bending moment at any point (x, y) due to the unit horizontal load at the crown is

$$m_H = -\frac{hx}{2r} + \frac{y}{2} = \frac{h}{2}\left(\frac{\cos \phi}{\cos \phi_1} - 1 + \frac{\sin \phi - \sin \phi_1}{1 - \sin \phi_1}\right) \tag{4.32}$$

For $\pi/2 \le \phi \le \pi$,

$$m_H = \frac{h}{2}\left(\frac{\cos \phi}{\text{coso } \phi_1} + 1 - \frac{\sin \phi - \sin \phi_1}{1 - \sin \phi_1}\right) \tag{4.33}$$

By application of virtual work, the displacement d_H of the crown to the right induced by the unit horizontal load is obtained from the summation over the arch rib

$$d_H = \sum_{1}^{1'} \frac{m_H{}^2 \, \Delta s}{EI} \tag{4.34}$$

Now, apply an upward vertical load P_V on rib $1C1'$ at (x_p, y_p), with the rib still disconnected from the other ribs. This produces the following reactions:

$$V_1 = -P_V \frac{2r - x}{2r} = -\frac{P_V}{2}\left(1 + \frac{\cos \phi_P}{\cos \phi_1}\right) \tag{4.35}$$

$$V_{1'} = -\frac{P_V}{2}\left(1 - \frac{\cos \phi_P}{\cos \phi_1}\right) \tag{4.36}$$

$$H_1 = -H_{1'} = V_{1'} \frac{r}{h} = -\frac{P_V}{2} \frac{\cos \phi_1 - \cos \phi_P}{1 - \sin \phi_1} \tag{4.37}$$

where ϕ_P is the angle that the radius vector to the load point (x_p, y_p) makes with the horizontal $\le \pi/2$. By application of virtual work, the horizontal and vertical components of the crown displacement induced by P_V may be computed from

$$\delta_{HV} = \sum_{1}^{1'} \frac{M_V m_H \, \Delta s}{EI} \tag{4.38}$$

$$\delta_{VV} = \sum_{1}^{1'} \frac{M_V m_V \, \Delta s}{EI} \tag{4.39}$$

where M_V is the bending moment produced at any point (x, y) by P_V.

Finally, apply a horizontal load P_H acting to the right on rib $1C1'$ at (x_P, y_P), with the rib still disconnected from the other ribs. This produces the following reactions:

$$V_{1'} = -V_1 = -P_H \frac{y}{2r} = -\frac{P_H}{2} \frac{\sin \phi_P - \sin \phi_1}{\cos \phi_1} \tag{4.40}$$

$$H_{1'} = -V_{1'} \frac{r}{h} = -\frac{P_H}{2} \frac{\sin \phi_P - \sin \phi_1}{1 - \sin \phi_1} \tag{4.41}$$

$$H_1 = -\frac{P_H}{2} \frac{2 - \sin \phi_1 - \sin \phi_P}{1 - \sin \phi_1} \tag{4.42}$$

By application of virtual work, the horizontal and vertical components of the crown displacement induced by P_H may be computed from

$$\delta_{HH} = \sum_{1}^{1'} \frac{M_H m_H \, \Delta s}{EI} \tag{4.43}$$

$$\delta_{VH} = \sum_{1}^{1'} \frac{M_H m_V \, \Delta s}{EI} \tag{4.44}$$

Displacement of the crown of rib $1C1'$, however, is resisted by a force X exerted at the crown by all the other ribs. Assume that X consists of an upward vertical force X_V and a horizontal force X_H acting to the left in the plane of $1C1'$. Equal but oppositely directed forces act at the junction of the other ribs.

Then the actual vertical displacement at the crown of rib $1C1'$ is

$$\delta_V = \delta_{VV} + \delta_{VH} - X_V d_V \tag{4.45}$$

Now, if V_r is the downward vertical force exerted at the crown of any other rib r, then the vertical displacement of that crown is

$$\delta_V = V_r d_V \tag{4.46}$$

Since the vertical displacements of the crowns of all ribs must be the same, the right-hand side of Eqs. (4.45) and (4.46) can be equated. Thus,

$$\delta_{VV} + \delta_{VH} - X_V d_V = V_r d_V = V_s d_V \tag{4.47}$$

where V_s is the vertical force exerted at the crown of another rib s. Hence

$$V_r = V_s \tag{4.48}$$

And for equilibrium at the crown,

$$X_V = \sum_{r=2}^{n} V_r = (n - 1)V_r \tag{4.49}$$

Substituting in Eq. (4.47) and solving for V_r yields

$$V_r = \frac{\delta_{VV} + \delta_{VH}}{n d_V} \tag{4.50}$$

The actual horizontal displacement at the crown of rib $1C1'$ is

$$\delta_H = \delta_{HV} + \delta_{HH} - X_H d_H \tag{4.51}$$

Now, if H_r is the horizontal force acting to the left at the crown of any other rib r, not perpendicular to rib $1C1'$, then the horizontal displacement of that crown parallel to the plane of rib $1C1'$ is

$$\delta_H = \frac{H_r d_H}{\cos \alpha_r} \tag{4.52}$$

Since for all ribs the horizontal crown displacements parallel to the plane of $1C1'$ must be the same, the right-hand side of Eqs. (4.51) and (4.52) can be equated. Hence

$$\delta_{HV} + \delta_{HH} - X_H d_H = \frac{H_r d_H}{\cos \alpha_r} = \frac{H_s d_H}{\cos \alpha_s} \tag{4.53}$$

where H_s is the horizontal force exerted on the crown of any other rib s and α_s is the angle between rib s and rib $1C1'$. Consequently,

$$H_s = H_r \frac{\cos \alpha_s}{\cos \alpha_r} \tag{4.54}$$

For equilibrium at the crown,

$$X_H = \sum_{s=2}^{n} H_s \cos \alpha_s = H_r \cos \alpha_r + \sum_{s=3}^{n} H_s \cos \alpha_s \tag{4.55}$$

Substitution of H_s as given by Eq. (4.54) in this equation gives

$$X_H = H_r \cos \alpha_r + \frac{H_r}{\cos \alpha_r} \sum_{s=3}^{n} \cos^2 \alpha_s = \frac{H_r}{\cos \alpha_r} \sum_{s=2}^{n} \cos^2 \alpha_s \tag{4.56}$$

Substituting this result in Eq. (4.53) and solving for H_r yields

$$H_r = \frac{\cos \alpha_r}{1 + \sum_{s=2}^{n} \cos^2 \alpha_s} \frac{\delta_{H'} + \delta_{H''}}{d_H} \tag{4.57}$$

Then, from Eq. (4.56),

$$X_H = \frac{\sum_{s=2}^{n} \cos^2 \alpha_s}{1 + \sum_{s=2}^{n} \cos^2 \alpha_s} \frac{\delta_{HV} + \delta_{HH}}{d_H} \tag{4.58}$$

Since X_V, X_H, V_r, and H_r act at the crown of the ribs, the reactions they induce can be determined by multiplication by the reactions for a unit load at the crown. For the unloaded ribs, the reactions thus computed are the actual reactions. For the loaded rib, the reactions should be superimposed on those computed for P_V from Eqs. (4.35) to (4.37) and for P_H from Eqs. (4.40) to (4.42).

Superimposition can be used to determine the reactions when several loads are applied simultaneously to one or more ribs.

Hemispherical Domes. For domes with ribs of constant moment of inertia and comprising a complete hemisphere, formulas for the reactions can be derived. These formulas may be useful in preliminary design of more complex domes.

If the radius of the hemisphere is R, the height h and radius r of the base of the dome also equal R. The coordinates of any point on rib $1C1'$ then are

$$x = R(1 - \cos \phi) \qquad y = R \sin \phi \qquad 0 \leq \phi \leq \frac{\pi}{2} \tag{4.59}$$

Assume temporarily that arch $1C1'$ is disconnected at the crown from all the other ribs. Apply a unit downward vertical load at the crown. This produces reactions

$$V_1 = V_{1'} = \tfrac{1}{2} \qquad H_1 = -H_{1'} = \tfrac{1}{2} \tag{4.60}$$

The bending moment at any point is

$$m_V = \frac{R}{2}(1 - \cos\phi - \sin\phi) \qquad 0 \le \phi \le \frac{\pi}{2} \tag{4.61a}$$

$$m_V = \frac{R}{2}(1 + \cos\phi - \sin\phi) \qquad \frac{\pi}{2} \le \phi \le \pi \tag{4.61b}$$

By application of virtual work, the downward vertical displacement d_V of the crown is

$$d_V = \int \frac{m_V^2\, ds}{EI} = \frac{R^3}{EI}\left(\frac{\pi}{2} - \frac{3}{2}\right) \tag{4.62}$$

Next, apply at the crown a unit horizontal load acting to the right. This produces reactions

$$V_1 = -V_{1'} = -\tfrac{1}{2} \qquad H_1 = H_{1'} = -\tfrac{1}{2} \tag{4.63}$$

The bending moment at any point is

$$m_H = \frac{R}{2}(\cos\phi - 1 + \sin\phi) \qquad 0 \le \phi \le \frac{\pi}{2} \tag{4.64a}$$

$$m_H = \frac{R}{2}(\cos\phi + 1 - \sin\phi) \qquad \frac{\pi}{2} \le \phi \le \pi \tag{4.64b}$$

By application of virtual work, the displacement of the crown d_H to the right is

$$d_H = \int \frac{m_H^2\, ds}{EI} = \frac{R^3}{EI}\left(\frac{\pi}{2} - \frac{3}{2}\right) \tag{4.65}$$

Now, apply an upward vertical load P_V on rib $1C1'$ at (x_P, y_P), with the rib still disconnected from the other ribs. This produces reactions

$$V_1 = -\frac{P_V}{2}(1 + \cos\phi_P) \tag{4.66}$$

$$V_{1'} = -\frac{P_V}{2}(1 - \cos\phi_P) \tag{4.67}$$

$$H_1 = H_{1'} = -\frac{P_V}{2}(1 - \cos\phi_P) \tag{4.68}$$

where $0 \le \phi_P \le \pi/2$. By application of virtual work, the vertical component of the crown displacement is

$$\delta_{VV} = \int \frac{M_V m_V\, ds}{EI} = \frac{P_V R^3}{EI} C_{VV} \tag{4.69}$$

$$C_{VV} = \frac{1}{4}\left(-\phi_P + 2\sin\phi_P - 3\cos\phi_P + \sin\phi_P\cos\phi_P - \sin^2\phi_P - 2\,\phi_P\cos\phi_P - 2\cos^2\phi_P + 5 - \frac{3\pi}{2} + \frac{3\pi}{2}\cos\phi_P\right) \tag{4.70}$$

For application to downward vertical loads, $-C_{VV}$ is plotted in Fig. 4.8. Similarly, the horizontal component of the crown displacement is

$$\delta_{HV} = \int \frac{M_V m_H \, ds}{EI} = \frac{P_V R^3}{EI} C_{HV} \tag{4.71}$$

$$C_{HV} = \frac{1}{4}\left(-\phi_P + 2 \sin \phi_P + 3 \cos \phi_P + \sin \phi_P \cos \phi_P - \sin^2 \phi_P - 2\phi_P \cos \phi_P - 2 \cos^2 \phi_P - 1 + \frac{\pi}{2} + \frac{\pi}{2} \cos \phi_P\right) \tag{4.72}$$

For application to downward vertical loads, $-C_{HV}$ is plotted in Fig. 4.8.

Finally, apply a horizontal load P_H acting to the right on rib $1C1'$ at (x_P, y_P), with the rib still disconnected from the other ribs. This produces reactions

$$V_1 = V_{1'} = \frac{P_H}{2} \sin \phi_P \tag{4.73}$$

$$H_1 = -P_H(1 - \tfrac{1}{2} \sin \phi_P) \tag{4.74}$$

$$H_{1'} = -\frac{P_H}{2} \sin \phi_P \tag{4.75}$$

By application of virtual work, the vertical component of the crown displacement is

$$\delta_{VH} = \int \frac{M_H m_V \, ds}{EI} = \frac{P_H R^3}{EI} C_{VH} \tag{4.76}$$

$$C_{VH} = \frac{1}{4}\left[-\phi_P + 3\left(\frac{\pi}{2} - 1\right) \sin \phi_P - 2 \cos \phi_P - \sin \phi_P \cos \phi_P + \sin^2 \phi_P - 2\phi_P \sin \phi_P + 2\right] \tag{4.77}$$

Values of C_{VH} are plotted in Fig. 4.8. The horizontal component of the displacement is

$$\delta_{HH} = \int \frac{M_H m_H \, ds}{EI} = \frac{P_H R^3}{EI} C_{HH} \tag{4.78}$$

$$C_{HH} = \frac{1}{4}\left[\phi_P + \left(\frac{\pi}{2} - 3\right) \sin \phi_P + 2 \cos \phi_P + \sin \phi_P \cos \phi_P - \sin^2 \phi_P + 2\phi_P \sin \phi_P - 2\right] \tag{4.79}$$

Values of C_{HH} also are plotted in Fig. 4.8.

For a vertical load P_V acting upward on rib $1C1'$, the forces exerted on the crown of an unloaded rib are, from Eqs. (4.50) and (4.57),

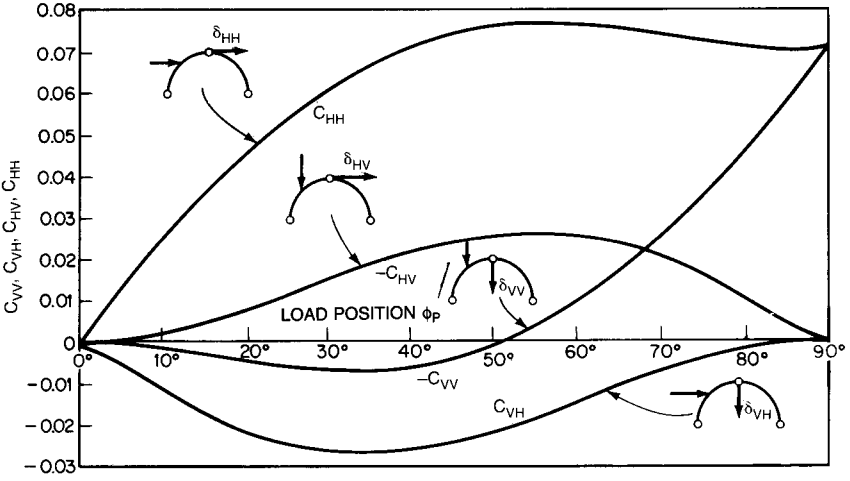

FIGURE 4.8 Coefficients for computing reactions of dome ribs.

$$V_r = \frac{\delta_{VH}}{nd_V} = \frac{2P_V C_{VH}}{n(\pi - 3)} \tag{4.80}$$

$$H_r = \frac{\delta_{HH}}{d_H}\beta \cos \alpha_r = -\frac{2P_V C_{HH}}{\pi - 3}\beta \cos \alpha_r \tag{4.81}$$

where $\beta = 1 \Big/ \left(1 + \sum_{s=2}^{n} \cos^2 \alpha_s\right)$

The reactions on the crown of the loaded rib are, from Eqs. (4.49) and (4.58),

$$X_V = (n - 1)V_r = \frac{n - 1}{n}\frac{2P_V C_{VV}}{\pi - 3} \tag{4.82}$$

$$X_H = \frac{\delta_{HV}}{d_H}\gamma = -\frac{2P_V C_{HV}}{\pi - 3} \tag{4.83}$$

where $\gamma = \beta \sum_{s=2}^{n} \cos^2 \alpha_s$

For a horizontal load P_H acting to the right on rib $1C1'$, the forces exerted on the crown of an unloaded rib are, from Eqs. (4.50) and (4.57),

$$V_r = \frac{\delta_{VH}}{nd_V} = \frac{2P_H C_{VH}}{n(\pi - 3)} \tag{4.84}$$

$$H_r = \frac{\delta_{HH}}{d_H}\beta \cos \alpha_r = \frac{2P_H C_{HH}}{\pi - 3}\beta \cos \alpha_r \tag{4.85}$$

The reactions on the crown of the loaded rib are, from Eqs. (4.49) and (4.58),

$$X_V = (n - 1)V_r = \frac{n - 1}{n} \frac{2P_H C_{VH}}{\pi - 3} \tag{4.86}$$

$$X_H = \frac{\delta_{HV}}{d_H} \gamma = \frac{2P_H C_{HH}}{\pi - 3} \gamma \tag{4.87}$$

The reactions for each rib caused by the crown forces can be computed with Eqs. (4.60) and (4.63). For the unloaded ribs, the actual reactions are the sums of the reactions caused by V_r and H_r. For the loaded rib, the reactions due to the load must be added to the sum of the reactions caused by X_V and X_H. The results are summarized in Table 4.2 for a unit vertical load acting downward ($P_V = -1$) and a unit horizontal load acting to the right ($P_H = 1$).

4.7 RIBBED AND HOOPED DOMES

Article 4.5 noted that domes may be thin-shelled, framed, or a combination. It also showed how thin-shelled domes can be analyzed. Article 4.6 showed how one type of framed dome, ribbed domes, can be analyzed. This article shows how to analyze another type, ribbed and hooped domes.

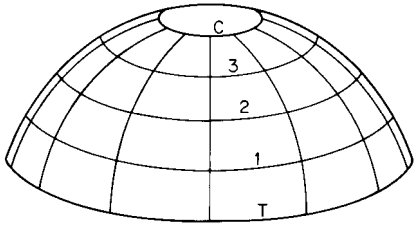

FIGURE 4.9 Ribbed and hooped dome.

This type also contains regularly spaced arch ribs around a closed horizontal curve. It also may have a tension ring around the base and a compression ring around the common crown. In addition, at regular intervals, the arch ribs are intersected by structural members comprising a ring, or hoop, around the dome in a horizontal plane (Fig. 4.9).

The rings resist horizontal displacement of the ribs at the points of intersection. If the rings are made sufficiently stiff, they may be considered points of support for the ribs horizontally. Some engineers prefer to assume the ribs hinged at those points. Others assume the ribs hinged only at tension and compression rings and continuous between those hoops. In many cases, the curvature of rib segments between rings may be ignored.

Figure 4.10*a* shows a rib segment 1–2 assumed hinged at the rings at points 1 and 2. A distributed downward load W induces bending moments between points 1 and 2 and shears assumed to be $W/2$ at 1 and 2. The ring segment above, 2–3, applied a thrust at 2 of $\Sigma W/\sin \theta_2$, where ΣW is the sum of the vertical loads on the rib from 2 to the crown and θ_2 is the angle with the horizontal of the tangent to the rib at 2.

These forces are resisted by horizontal reactions at the rings and a tangential thrust, provided by a rib segment below 1 or an abutment at 1. For equilibrium, the vertical component of the thrust must equal $W + \Sigma W$. Hence the thrust equals $(W + \Sigma W)/\sin \theta_1$, where θ_1 is the angle with the horizontal of the tangent to the rib at 1.

Setting the sum of the moments about 1 equal to zero yields the horizontal reaction supplied by the ring at 2:

$$H_2 = \frac{WL_H}{2L_V} + \frac{L_H}{L_V} \Sigma W - (\Sigma W) \cot \theta_2 \tag{4.88}$$

where L_H = horizontal distance between 1 and 2
L_V = vertical distance between 1 and 2

Setting the sum of the moments about 2 equal to zero yields the horizontal reaction supplied by the ring at 1:

TABLE 4.2 Reactions of Ribs of Hemispherical Ribbed Dome

$$\pi = \frac{1}{1 + \sum_{s=2}^{n} \cos^2 \alpha_s} \qquad \gamma = \beta \sum_{s=2}^{n} \cos^2 \alpha_s$$

ϕ_P = angle the radius vector to load from center of hemisphere makes with horizontal

α_r = angle between loaded and unloaded rib $\leq \pi/2$

Reactions of loaded rib Unit downward vertical load	**Reactions of unloaded rib** Unit downward vertical load
$V_1 = \frac{1}{2} + \frac{1}{2}\cos\phi_P - \frac{n-1}{n}\frac{C_{VV}}{\pi - 3} + \frac{C_{HV}}{\pi - 3}\gamma$	$V_r = \frac{C_{VV}}{n(\pi - 3)} - \frac{C_{HV}}{\pi - 3}\beta\cos\alpha_r$
$V_{1'} = \frac{1}{2} - \frac{1}{2}\cos\phi_P - \frac{n-1}{n}\frac{C_{VV}}{\pi - 3} - \frac{C_{HV}}{\pi - 3}\gamma$	$V_{r'} = \frac{C_{VV}}{n(\pi - 3)} + \frac{C_{HV}}{\pi - 3}\beta\cos\alpha_r$
$H_1 = \frac{1}{2} - \frac{1}{2}\cos\phi_P - \frac{n-1}{n}\frac{C_{VV}}{\pi - 3} + \frac{C_{HV}}{\pi - 3}\gamma$	$H_r = \frac{C_{VV}}{n(\pi - 3)} - \frac{C_{HV}}{\pi - 3}\beta\cos\alpha_r$
$H_{1'} = -\frac{1}{2} + \cos\phi_P + \frac{n-1}{n}\frac{C_{VV}}{\pi - 3} + \frac{C_{HV}}{\pi - 3}\gamma$	$H_{r'} = -\frac{C_{VV}}{n(\pi - 3)} - \frac{C_{HV}}{\pi - 3}\beta\cos\alpha_r$
Unit horizontal load acting to right	Unit horizontal load acting to right
$V_1 = -\frac{1}{2}\sin\phi_P - \frac{n-1}{n}\frac{C_{VH}}{\pi - 3} + \frac{C_{HH}}{\pi - 3}\gamma$	$V_r = \frac{C_{VH}}{n(\pi - 3)} - \frac{C_{HH}}{\pi - 3}\beta\cos\alpha_r$
$V_{1'} = \frac{1}{2}\sin\phi_P - \frac{n-1}{n}\frac{C_{VH}}{\pi - 3} - \frac{C_{HH}}{\pi - 3}\gamma$	$V_{r'} = \frac{C_{VH}}{n(\pi - 3)} + \frac{C_{HH}}{\pi - 3}\beta\cos\alpha_r$
$H_1 = -1 + \frac{1}{2}\sin\phi_P - \frac{n-1}{n}\frac{C_{VH}}{\pi - 3} + \frac{C_{HH}}{\pi - 3}\gamma$	$H_r = \frac{C_{VH}}{n(\pi - 3)} - \frac{C_{HH}}{\pi - 3}\beta\cos\alpha_r$
$H_{1'} = -\frac{1}{2}\sin\phi_P + \frac{n-1}{n}\frac{C_{VH}}{\pi - 3} + \frac{C_{HH}}{\pi - 3}\gamma$	$H_{r'} = -\frac{C_{VH}}{n(\pi - 3)} - \frac{C_{HH}}{\pi - 3}\beta\cos\alpha_r$

$$H_1 = \frac{W}{2}\left(\frac{L_H}{L_V} - 2\cot\theta_1\right) + \left(\frac{L_H}{L_V} - \cot\theta_1\right)\Sigma W \tag{4.89}$$

For the direction assumed for H_2, the ring at 2 will be in compression when the right-hand side of Eq. (4.88) is positive. Similarly, for the direction assumed for H_1, the ring at 1 will be in tension when the right-hand side of Eq. (4.89) is positive. Thus the type of stress in the rings depends on the relative values of L_H/L_V and cot θ_1 or cot θ_2. Alternatively, it depends on the difference in the slope of the thrust at 1 or 2 and the slope of the line from 1 to 2.

Generally, for maximum stress in the compression ring about the crown or tension ring around the base, a ribbed and hooped dome should be completely loaded with full dead and

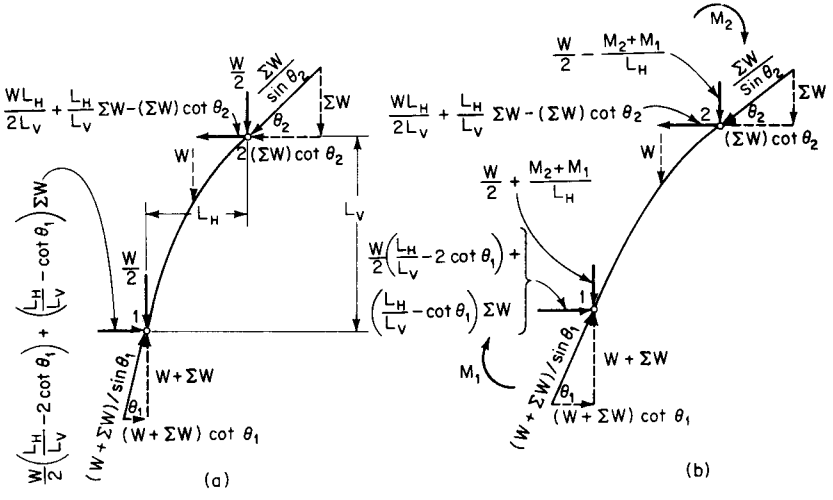

FIGURE 4.10 Forces acting on a segment of a dome rib between hoops. (*a*) Ends of segment assumed hinged. (*b*) Rib assumed continuous.

live loads. For an intermediate ring, maximum tension will be produced with live load extending from the ring to the crown. Maximum compression will result when the live load extends from the ring to the base.

When the rib is treated as continuous between crown and base, moments are introduced at the ends of each rib segment (Fig. 4.l0*b*). These moments may be computed in the same way as for a continuous beam on immovable supports, neglecting the curvature of rib between supports. The end moments affect the bending moments between points 1 and 2 and the shears there, as indicated in Fig. 4. l0*b*. But the forces on the rings are the same as for hinged rib segments.

The rings may be analyzed by elastic theory in much the same way as arches. Usually, however, for loads on the ring segments between ribs, these segments are treated as simply supported or fixed-end beams. The hoop tension or thrust T may be determined, as indicated in Fig. 4.11 for a circular ring, by the requirements of equilibrium:

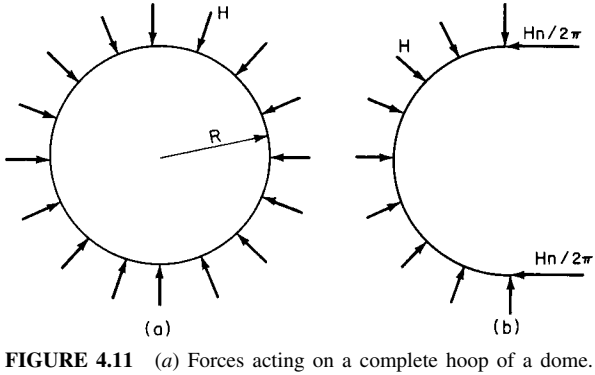

FIGURE 4.11 (*a*) Forces acting on a complete hoop of a dome. (*b*) Forces acting on half of a hoop.

$$T = \frac{Hn}{2\pi} \tag{4.90}$$

where H = radial force exerted on ring by each rib
n = number of load points

The procedures outlined neglect the effects of torsion and of friction in joints, which could be substantial. In addition, deformations of such domes under overloads often tend to redistribute those loads to less highly loaded members. Hence more complex analyses without additional information on dome behavior generally are not warranted.

Many domes have been constructed as part of a hemisphere, such that the angle made with the horizontal by the radius vector from the center of the sphere to the base of the dome is about 60°. Thus the radius of the sphere is nearly equal to the diameter of the dome base, and the rise-to-span ratio is about $1 - \sqrt{3}/2$, or 0.13. Some engineers believe that high structural economy results with such proportions.

(Z. S. Makowski, *Analysis, Design, and Construction of Braced Domes,* Granada Technical Books, London, England.)

4.8 SCHWEDLER DOMES

An interesting structural form, similar to the ribbed and hooped domes described in Section 4.7 is the Schwedler Dome. In this case, the dome is composed of two force members arranged as the ribs and hoops along with a single diagonal in each of the resulting panels, as shown in Fig. 4.12. Although the structural form looks complex, the structure is determinate and exhibits some interesting characteristics.

The application of the equations of equilibrium available for three dimensional, pinned structures will verify that the Schwedler Dome is a determinate structure. In addition, the application of three special theorems will allow for a significant reduction in the amount of computational effort required for the analysis. These theorems may be stated as:

1. If all members meeting at a joint with the exception of one, lie in a plane, the component normal to the plane of the force in the bar is equal to the component normal to the plane of any load applied to the joint,
2. If all the members framing into a joint, with the exception of one, are in the same plane and there are no external forces at the joint, the force in the member out of the plane is zero, and
3. If all but two members meeting at a joint have zero force, the two remaining members are not collinear, and there is no externally applied force, the two members have zero force.

A one panel high, square base Schwedler Dome is shown in Fig. 4.13. The base is supported with vertical reactions at all four corners and in the plane of the base as shown. The structure will be analyzed for a vertical load applied at A.

At joint B, the members BA, BE, and BF lie in a plane, but BC does not. Since there is no load applied to joint B, the application of Theorem 2 indicates that member BC would have zero force. Proceeding around the top of the structure to joints C and D respectively will show that the force in member CD (at C), and DA (at D) are both zero.

Now Theorem 3 may be applied at joints C and D since in both cases, there are only two members remaining at each joint and there is no external load. This results in the force in members CF, CG, DG, and DH being zero. The forces in the remaining members may be determined by the application of the method of joints.

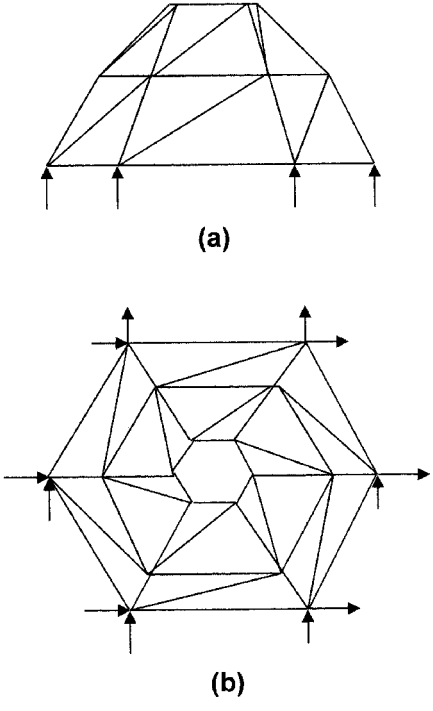

FIGURE 4.12 Schwedler dome. (a) Elevation. (b) Plan.

Note that the impact of the single concentrated force applied at joint *A* is restricted to a few select members. If loads are applied to the other joints in the top plane, the structure could easily be analyzed for each force independently with the results superimposed. Regardless of the number of base sides in the dome or the number of panels of height, the three theorems will apply and yield a significantly reduced number of members actually carrying load. Thus, the effort required to fully analyze the Schwedler Dome is also reduced.

4.9 SIMPLE SUSPENSION CABLES

The objective of this and the following article is to present general procedures for analyzing simple cable suspension systems. The numerous types of cable systems available make it impractical to treat anything but the simplest types. Additional information may be found in Sec. 15, which covers suspension bridges and cable-stayed structures.

Characteristics of Cables. A **suspension cable** is a linear structural member that adjusts its shape to carry loads. The primary assumptions in the analysis of cable systems are that the cables carry only tension and that the tension stresses are distributed uniformly over the cross section. Thus no bending moments can be resisted by the cables.

For a cable subjected to gravity loads, the equilibrium positions of all points on the cable may be completely defined, provided the positions of any three points on the cable are

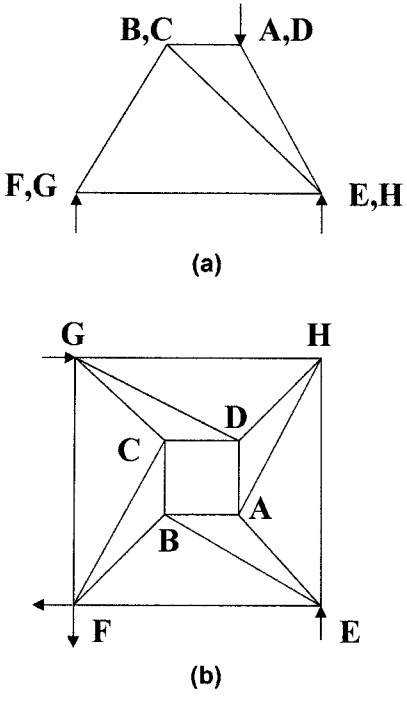

FIGURE 4.13 Example problem for Schwedler dome. (a) Elevation. (b) Plan.

known. These points may be the locations of the cable supports and one other point, usually the position of a concentrated load or the point of maximum sag. For gravity loads, the shape of a cable follows the shape of the moment diagram that would result if the same loads were applied to a simple beam. The maximum sag occurs at the point of maximum moment and zero shear for the simple beam.

The tensile force in a cable is tangent to the cable curve and may be described by horizontal and vertical components. When the cable is loaded only with gravity loads, the horizontal component at every point along the cable remains constant. The maximum cable force will occur where the maximum vertical component occurs, usually at one of the supports, while the minimum cable force will occur at the point of maximum sag.

Since the geometry of a cable changes with the application of load, the common approaches to structural analysis, which are based on small-deflection theories, will not be valid, nor will superposition be valid for cable systems. In addition, the forces in a cable will change as the cable elongates under load, as a result of which equations of equilibrium are nonlinear. A common approximation is to use the linear portion of the exact equilibrium equations as a first trial and to converge on the correct solution with successive approximations.

A cable must satisfy the second-order linear differential equation

$$Hy'' = q \tag{4.91}$$

where H = horizontal force in cable
y = rise of cable at distance x from low point (Fig. 4.14)

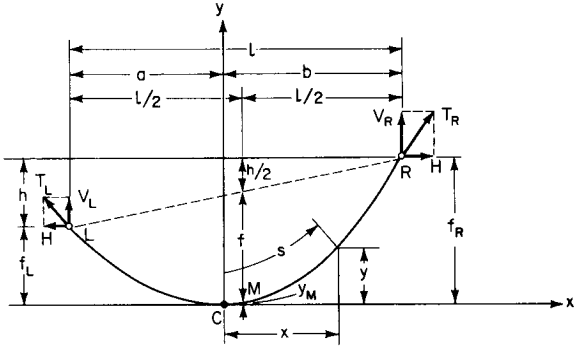

FIGURE 4.14 Cable with supports at different levels.

$y'' = d^2y/dx^2$
q = gravity load per unit span

4.9.1 Catenary

Weight of a cable of constant cross section represents a vertical loading that is uniformly distributed along the length of cable. Under such a loading, a cable takes the shape of a catenary.

To determine the stresses in and deformations of a catenary, the origin of coordinates is taken at the low point C, and distance s is measured along the cable from C (Fig. 4.14). With q_o as the load per unit length of cable, Eq. (4.91) becomes

$$Hy'' = \frac{q_o\, ds}{dx} = q_o \sqrt{1 + y'^2} \tag{4.92}$$

where $y' = dy/dx$. Solving for y' gives the slope at any point of the cable:

$$y' = \frac{\sinh q_o x}{H} = \frac{q_o x}{H} + \frac{1}{3!}\left(\frac{q_o x}{H}\right)^3 + \cdots \tag{4.93}$$

A second integration then yields

$$y = \frac{H}{q_o}\left(\cosh \frac{q_o x}{H} - 1\right) = \frac{q_o}{H}\frac{x^2}{2!} + \left(\frac{q_o}{H}\right)^3 \frac{x^4}{4!} + \cdots \tag{4.94}$$

Equation (4.94) is the catenary equation. If only the first term of the series expansion is used, the cable equation represents a parabola. Because the parabolic equation usually is easier to handle, a catenary often is approximated by a parabola.

For a catenary, length of arc measured from the low point is

$$s = \frac{H}{q_o} \sinh \frac{q_o x}{H} = x + \frac{1}{3!}\left(\frac{q_o}{H}\right)^2 x^3 + \cdots \tag{4.95}$$

Tension at any point is

$$T = \sqrt{H^2 + q_o^2 s^2} = H + q_o y \tag{4.96}$$

The distance from the low point C to the left support L is

$$a = \frac{H}{q_o} \cosh^{-1} \left(\frac{q_o}{H} f_L + 1 \right) \tag{4.97}$$

where f_L is the vertical distance from C to L. The distance from C to the right support R is

$$b = \frac{H}{q_o} \cosh^{-1} \left(\frac{q_o}{H} f_R + 1 \right) \tag{4.98}$$

where f_R is the vertical distance from C to R.

Given the sags of a catenary f_L and f_R under a distributed vertical load q_o, the horizontal component of cable tension H may be computed from

$$\frac{q_o l}{H} = \cosh^{-1} \left(\frac{q_o f_L}{H} + 1 \right) + \cosh^{-1} \left(\frac{q_o f_R}{H} + 1 \right) \tag{4.99}$$

where l is the span, or horizontal distance, between supports L and $R = a + b$. This equation usually is solved by trial. A first estimate of H for substitution in the right-hand side of the equation may be obtained by approximating the catenary by a parabola. Vertical components of the reactions at the supports can be computed from

$$R_L = \frac{H \sinh q_o a}{H} \qquad R_R = \frac{H \sinh q_o b}{H} \tag{4.100}$$

See also Art. 14.6.

4.9.2 Parabola

Uniform vertical live loads and uniform vertical dead loads other than cable weight generally may be treated as distributed uniformly over the horizontal projection of the cable. Under such loadings, a cable takes the shape of a parabola.

To determine cable stresses and deformations, the origin of coordinates is taken at the low point C (Fig. 4.14). With w_o as the uniform load on the horizontal projection, Eq. (4.91) becomes

$$Hy'' = w_o \tag{4.101}$$

Integration gives the slope at any point of the cable:

$$y' = \frac{w_o x}{H} \tag{4.102}$$

A second integration then yields the parabolic equation

$$y = \frac{w_o x^2}{2H} \tag{4.103}$$

The distance from the low point C to the left support L is

$$a = \frac{l}{2} - \frac{Hh}{w_o l} \tag{4.104}$$

where l = span, or horizontal distance, between supports L and $R = a + b$
h = vertical distance between supports

The distance from the low point C to the right support R is

$$b = \frac{l}{2} + \frac{Hh}{w_o l} \tag{4.105}$$

When supports are not at the same level, the horizontal component of cable tension H may be computed from

$$H = \frac{w_o l^2}{h^2}\left(f_R - \frac{h}{2} \pm \sqrt{f_L f_R}\right) = \frac{w_o l^2}{8f} \tag{4.106}$$

where f_L = vertical distance from C to L
f_R = vertical distance from C to R
f = sag of cable measured vertically from chord LR midway between supports (at $x = Hh/w_o l$)

As indicated in Fig. 4.14,

$$f = f_L + \frac{h}{2} - y_M \tag{4.107}$$

where $y_M = Hh^2/2w_o l^2$. The minus sign should be used in Eq. (4.106) when low point C is between supports. If the vertex of the parabola is not between L and R, the plus sign should be used.

The vertical components of the reactions at the supports can be computed from

$$V_L = w_o a = \frac{w_o l}{2} - \frac{Hh}{l} \quad V_R = w_o b = \frac{w_o l}{2} + \frac{Hh}{l} \tag{4.108}$$

Tension at any point is

$$T = \sqrt{H^2 + w_o{}^2 x^2}$$

Length of parabolic arc RC is

$$L_{RC} = \frac{b}{2}\sqrt{1 + \left(\frac{w_o b}{H}\right)^2} + \frac{H}{2w_o}\sinh\frac{w_{ob}}{H} = b + \frac{1}{6}\left(\frac{w_o}{\mathrm{H}}\right)^2 b^3 + \cdots \tag{4.109}$$

Length of parabolic arc LC is

$$L_{LC} = \frac{a}{2}\sqrt{1 + \left(\frac{w_o a}{H}\right)^2} + \frac{H}{2w_o}\sinh\frac{w_o a}{H} = a + \frac{1}{6}\left(\frac{w_o}{H}\right)^2 a^3 + \cdots \tag{4.110}$$

When supports are at the same level, $f_L = f_R = f$, $h = 0$, and $a = b = 1/2$. The horizontal component of cable tension H may be computed from

$$H = \frac{w_o l^2}{8f} \tag{4.111}$$

The vertical components of the reactions at the supports are

$$V_L = V_R = \frac{w_o l}{2} \tag{4.112}$$

Maximum tension occurs at the supports and equals

$$T_L = T_R = \frac{w_o l}{2}\sqrt{1 + \frac{l^2}{16f^2}} \tag{4.113}$$

Length of cable between supports is

$$L = \frac{l}{2}\sqrt{1 + \left(\frac{w_o l}{2H}\right)^2} + \frac{H}{w_o}\sinh\frac{w_o l}{2H}$$
$$= l\left(1 + \frac{8}{3}\frac{f^2}{l^2} - \frac{32}{5}\frac{f^4}{l^4} + \frac{256}{7}\frac{f^6}{l^6} + \cdots\right) \tag{4.114}$$

If additional uniformly distributed load is applied to a parabolic cable, the elastic elongation is

$$\Delta L = \frac{Hl}{AE}\left(1 + \frac{16}{3}\frac{f^2}{l^2}\right) \tag{4.115}$$

where A = cross-sectional area of cable
E = modulus of elasticity of cable steel
H = horizontal component of tension in cable

The change in sag is approximately

$$\Delta f = \frac{15}{16}\frac{l}{f}\left(\frac{\Delta L}{5 - 24f^2/l^2}\right) \tag{4.116}$$

If the change is small and the effect on H is negligible, this change may be computed from

$$\Delta f = \frac{15}{16}\frac{Hl^2}{AEf}\left(\frac{1 + 16f^2/3l^2}{5 - 24f^2/l^2}\right) \tag{4.117}$$

For a rise in temperature t, the change in sag is about

$$\Delta f = \frac{15}{16}\frac{l^2 ct}{f(5 - 24f^2/l^2)}\left(1 + \frac{8}{3}\frac{f^2}{l^2}\right) \tag{4.118}$$

where c is the coefficient of thermal expansion.

4.9.3 Example—Simple Cable

A cable spans 300 ft and supports a uniformly distributed load of 0.2 kips per ft. The unstressed equilibrium configuration is described by a parabola with a sag at the center of the span of 20 ft. $A = 1.47$ in^2 and $E = 24{,}000$ ksi. Successive application of Eqs. (4.111), (4.115), and (4.116) results in the values shown in Table 4.3. It can be seen that the process converges to a solution after five cycles.

(H. Max Irvine, *Cable Structures,* MIT Press, Cambridge, Mass.; Prem Krishna, *Cable-Suspended Roofs,* McGraw-Hill, Inc., New York; J. B. Scalzi et al., *Design Fundamentals of Cable Roof Structures,* U.S. Steel Corp., Pittsburgh, Pa.; J. Szabo and L. Kollar, *Structural Design of Cable-Suspended Roofs,* Ellis Horwood Limited, Chichester, England.)

TABLE 4.3 Example Cable Problem

Cycle	Sag, ft	Horizontal force, kips, from Eq. (4.111)	Change in length, ft, from Eq. (4.115)	Change in sag, ft. from Eq. (4.116)	New sag, ft
1	20.00	112.5	0.979	2.81	22.81
2	22.81	98.6	0.864	2.19	22.19
3	22.19	101.4	0.887	2.31	22.31
4	22.31	100.8	0.883	2.29	22.29
5	22.29	100.9	0.884	2.29	22.29

4.10 CABLE SUSPENSION SYSTEMS

Single cables, such as those analyzed in Art. 4.9, have a limited usefulness when it comes to building applications. Since a cable is capable of resisting only tension, it is limited to transferring forces only along its length. The vast majority of structures require a more complex ability to transfer forces. Thus it is logical to combine cables and other load-carrying elements into systems. Cables and beams or trusses are found in combination most often in suspension bridges (see Sec. 15), while for buildings it is common to combine multiple cables into cable systems, such as three-dimensional networks or two-dimensional cable beams and trusses.

Like simple cables, cable systems behave nonlinearly. Thus accurate analysis is difficult, tedious, and time-consuming. As a result, many designers use approximate methods or preliminary designs that appear to have successfully withstood the test of time. Because of the numerous types of systems and the complexity of analysis, only general procedures will be outlined in this article, which deals with cable systems in which the loads are carried to supports only by cables.

Networks consist of two or three sets of parallel cables intersecting at an angle. The cables are fastened together at their intersections. **Cable trusses** consist of pairs of cables, generally in a vertical plane. One cable of each pair is concave downward, the other concave upward (Fig. 4.15). The two cables of a cable truss play different roles in carrying load. The sagging cable, whether it is the upper cable (Fig. 4.15*a* or *b*), the lower cable (Fig. 14.15*d*), or in both positions (Fig. 4.15*c*), carries the gravity load, while the rising cable resists upward load and provides damping. Both cables are initially tensioned, or prestressed, to a predetermined shape, usually parabolic. The prestress is made large enough that any compression that may be induced in a cable by superimposed loads only reduces the tension in the cable;

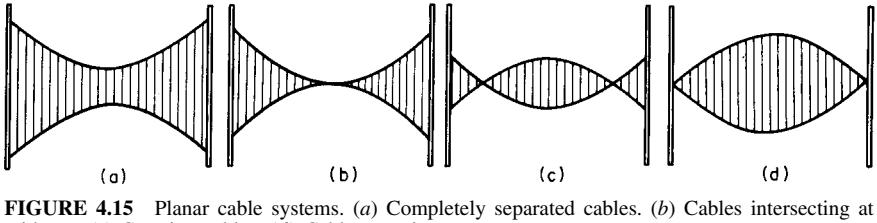

FIGURE 4.15 Planar cable systems. (*a*) Completely separated cables. (*b*) Cables intersecting at midspan. (*c*) Crossing cables. (*d*) Cables meeting at supports.

thus compressive stresses cannot occur. The relative vertical position of the cables is maintained by vertical spreaders or by diagonals. Diagonals in the truss plane do not appear to increase significantly the stiffness of a cable truss.

Figure 4.15 shows four different arrangements of cables with spreaders to form a cable truss. The intersecting types (Fig. 4.15*b* and *c*) usually are stiffer than the others, for given size cables and given sag and rise.

For supporting roofs, cable trusses often are placed radially at regular intervals. Around the perimeter of the roof, the horizontal component of the tension usually is resisted by a circular or elliptical compression ring. To avoid a joint with a jumble of cables at the center, the cables usually are also connected to a tension ring circumscribing the center.

Cable trusses may be analyzed as discrete or continuous systems. For a discrete system, the spreaders are treated as individual members and the cables are treated as individual members between each spreader. For a continuous system, the spreaders are replaced by a continuous diaphragm that ensures that the changes in sag and rise of cables remain equal under changes in load.

To illustrate the procedure for a cable truss treated as a continuous system, the type shown in Fig. 4.15*d* and again in Fig. 4.16 will be analyzed. The bottom cable will be the load-carrying cable. Both cables are prestressed and are assumed to be parabolic. The horizontal component H_{iu} of the initial tension in the upper cable is given. The resulting rise is f_u, and the weight of cables and spreaders is taken as w_c. Span is l.

The horizontal component of the prestress in the bottom cable H_{ib} can be determined by equating the bending moment in the system at midspan to zero:

$$H_{ib} = \frac{f_u}{f_b} H_{iu} + \frac{w_c l^2}{8 f_b} = \frac{(w_c + w_i) l^2}{8 f_b} \tag{4.119}$$

where f_b = sag of lower cable
w_i = uniformly distributed load exerted by diaphragm on each cable when cables are parabolic

Setting the bending moment at the high point of the upper cable equal to zero yields

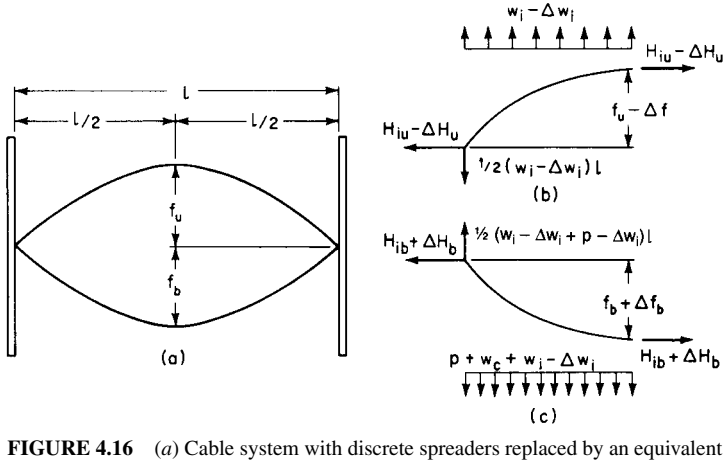

FIGURE 4.16 (*a*) Cable system with discrete spreaders replaced by an equivalent diaphragm. (*b*) Forces acting on the top cable. (*c*) Forces acting on the bottom cable.

$$w_i = \frac{8H_{iu}f_u}{l^2} \tag{4.120}$$

Thus the lower cable carries a uniform downward load $w_c + w_i$, while the upper cable is subjected to a distributed upward force w_i.

Suppose a load p uniformly distributed horizontally is now applied to the system (Fig. 4.16*a*). This load may be dead load or dead load plus live load. It will decrease the tension in the upper cable by ΔH_u and the rise by Δf (Fig. 4.16*b*). Correspondingly, the tension in the lower cable will increase by ΔH_b and the sag by Δf (Fig. 4.16*c*). The force exerted by the diaphragm on each cable will decrease by Δw_i.

The changes in tension may be computed from Eq. (4.117). Also, application of this equation to the bending-moment equations for the midpoints of each cable and simultaneous solution of the resulting pair of equations yields the changes in sag and diaphragm force. The change in sag may be estimated from

$$\Delta f = \frac{1}{H_{iu} + H_{ib} + (A_u f_u^2 + A_b f_b^2)16E/3l^2} \frac{pl^2}{8} \tag{4.121}$$

where A_u = cross-sectional area of upper cable
A_b = cross-sectional area of lower cable

The decrease in uniformly distributed diaphragm force is given approximately by

$$\Delta w_i = \frac{(H_{iu} + 16A_u E f_u^2/3l^2)p}{H_{iu} + H_{ib} + (A_u f_u^2 + A_b f_b^2)16E/3l^2} \tag{4.122}$$

And the change in load on the lower cable is nearly

$$p - \Delta w_i = \frac{(H_{ib} + 16A_b E f_b^2/3l^2)p}{H_{iu} + H_{ib} + (A_u f_u^2 + A_b f_b^2)16E/3l^2} \tag{4.123}$$

In Eqs. (4.121) to (4.123), the initial tensions H_{iu} and H_{ib} generally are relatively small compared with the other terms and can be neglected. If then $f_u = f_b$, as is often the case, Eq. (4.122) simplifies to

$$\Delta w_i = \frac{A_u}{A_u + A_b} p \tag{4.124}$$

and Eq. (4.123) becomes

$$p - \Delta w_i = \frac{A_b}{A_u + A_b} p \tag{4.125}$$

The horizontal component of tension in the upper cable for load p may be computed from

$$H_u = H_{iu} - \Delta H_u = \frac{w_i - \Delta w_i}{w_i} H_{iu} \tag{4.126}$$

The maximum vertical component of tension in the upper cable is

$$V_u = \frac{(w_i - \Delta w_i)l}{2} \tag{4.127}$$

The horizontal component of tension in the lower cable may be computed from

$$H_b = H_{ib} + \Delta H_b = \frac{w_c + w_i + p - \Delta w_i}{w_c + w_i} H_{ib} \tag{4.128}$$

The maximum vertical component of tension in the lower cable is

$$V_b = \frac{(w_c + w_i + p - \Delta w_i)l}{2} \tag{4.129}$$

In general, in analysis of cable systems, terms of second-order magnitude may be neglected, but changes in geometry should not be ignored.

Treatment of a cable truss as a discrete system may be much the same as that for a cable network considered a discrete system. For loads applied to the cables between joints, or nodes, the cable segments between nodes are assumed parabolic. The equations given in Art. 4.9 may be used to determine the forces in the segments and the forces applied at the nodes. Equilibrium equations then can be written for the forces at each joint.

These equations, however, generally are not sufficient for determination of the forces acting in the cable system. These forces also depend on the deformed shape of the network. They may be determined from equations for each joint that take into account both equilibrium and displacement conditions.

For a cable truss (Fig. 4.16*a*) prestressed initially into parabolic shapes, the forces in the cables and spreaders can be found from equilibrium conditions, as indicated in Fig. 4.17. With the horizontal component of the initial tension in the upper cable H_{iu} given, the prestress in the segment to the right of the high point of that cable (joint 1, Fig. 4.17*a*) is $T_{iu1} = H_{iu}/\cos \alpha_{Ru1}$. The vertical component of this tension equals $W_{i1} - W_{cu1}$, where W_{i1} is the force exerted by the spreader and W_{cu1} is the load on joint 1 due to the weight of the upper cable. (If the cable is symmetrical about the high point, the vertical component of tension in the cable segment is $(W_{i1} - W_{xu1})/2$.] The direction cosine of the cable segment cos α_{Ru1} is determined by the geometry of the upper cable after it is prestressed. Hence W_{i1} can be computed readily when H_{iu} is known.

With W_{i1} determined, the initial tension in the lower cable at its low point (joint 1, Fig, 4.17*c*) can be found from equilibrium requirements in similar fashion and by setting the

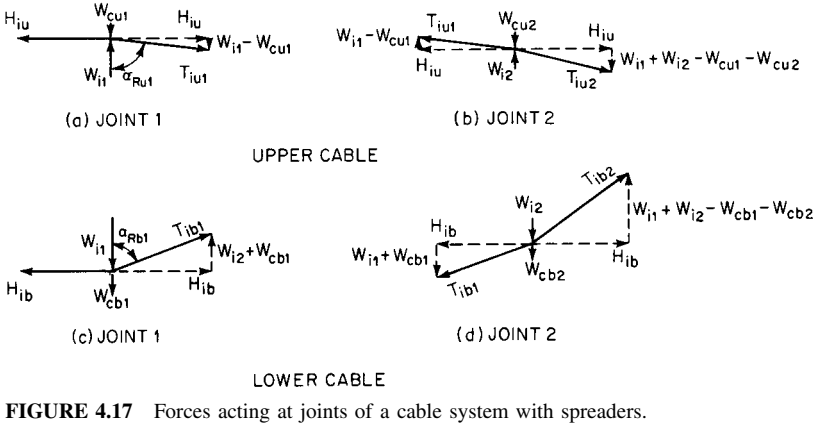

FIGURE 4.17 Forces acting at joints of a cable system with spreaders.

bending moment at the low point equal to zero. Similarly, the cable and spreader forces at adjoining joints (joint 2, Fig. 4.17*b* and *d*) can be determined.

Suppose now vertical loads are applied to the system. They can be resolved into concentrated vertical loads acting at the nodes, such as the load P at a typical joint O_b of the bottom cable, shown in Fig. 4.18*b*. The equations of Art. 4.9 can be used for the purpose. The loads will cause vertical displacements δ of all the joints. The spreaders, however, ensure that the vertical displacement of each upper-cable node equals that of the lower-cable node below. A displacement equation can be formulated for each joint of the system. This equation can be obtained by treating a cable truss as a special case of a cable network.

A cable network, as explained earlier, consists of interconnected cables. Let joint O in Fig. 4.18*a* represent a typical joint in a cable network and 1, 2, 3. . . . adjoining joints. Cable segments $O1$, $O2$, $O3$. . . . intersect at O. Joint O is selected as the origin of a three-dimensional, coordinate system.

In general, a typical cable segment Or will have direction cosines $\cos \alpha_{rx}$ with respect to the x axis, $\cos \alpha_{ry}$ with respect to the y axis, and $\cos \alpha_{rz}$ with respect to the z axis. A load P at O can be resolved into components P_x parallel to the x axis, P_y parallel to the y axis, and P_z parallel to the z axis. Similarly, the displacement of any joint r can be resolved into components δ_{rx}, δ_{ry}, and δ_{rz}. For convenience, let

$$\Delta_x = \delta_{rx} - \delta_{0x} \qquad \Delta_y = \delta_{ry} - \delta_{0y} \qquad \Delta_z = \delta_{rz} - \delta_{0z} \tag{4.130}$$

For a cable-network joint, in general, then, where n cable segments interconnect, three equations can be established:

$$\sum_{r=1}^{n} \left[\frac{EA_r}{l_r} \cos \alpha_{rz} (\Delta_x \cos \alpha_{rx} + \Delta_y \cos \alpha_{ry} + \Delta_z \cos \alpha_{rz}) \right] + P_z = 0 \tag{4.131a}$$

$$\sum_{r=1}^{n} \left[\frac{EA_r}{l_r} \cos \alpha_{ry} (\Delta_x \cos \alpha_{rx} + \Delta_y \cos \alpha_{ry} + \Delta_z \cos \alpha_{rz}) \right] + P_y = 0 \tag{4.131b}$$

$$\sum_{r=1}^{n} \left[\frac{EA_r}{l_r} \cos \alpha_{rx} (\Delta_x \cos \alpha_{rx} + \Delta_y \cos \alpha_{ry} + \Delta_z \cos \alpha_{rz}) \right] + P_x = 0 \tag{4.131c}$$

where E = modulus of elasticity of steel cable
A_r = cross-sectional area of cable segment Or
l_r = length of chord from O to r

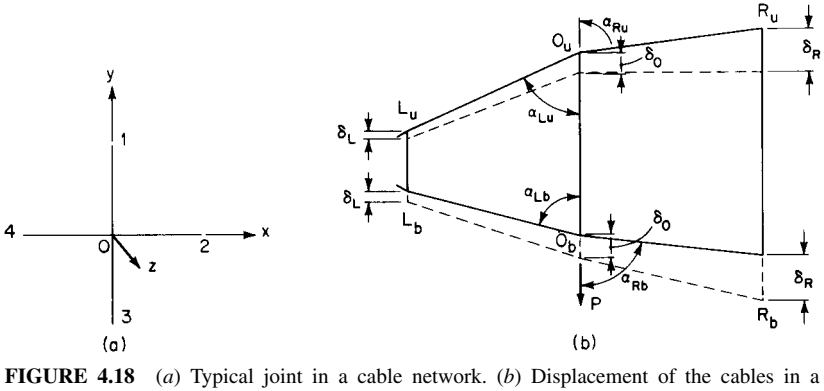

FIGURE 4.18 (*a*) Typical joint in a cable network. (*b*) Displacement of the cables in a network caused by a load acting at a joint.

These equations are based on the assumption that deflections are small and that, for any cable segment, initial tension T_i can be considered negligible compared with EA.

For a cable truss, $n = 2$ for a typical joint. If only vertical loading is applied, only Eq. (4.131*a*) is needed. At typical joints O_u of the upper cable and O_b of the bottom cable (Fig. 4.18*b*), the vertical displacement is denoted by δ_o. The displacements of the joints L_u and L_b on the left of O_u and O_b are indicated by δ_L. Those of the joints R_u and R_b on the right of O_u and O_b are represented by δ_R. Then, for joint O_u, Eq. (4.131*a*) becomes

$$\frac{EA_{Lu}}{l_{Lu}} \cos^2 \alpha_{Lu}(\delta_L - \delta_O) + \frac{EA_{Ru}}{l_{Ru}} \cos^2 \alpha_{Ru}(\delta_R - \delta_O) = W_i - \Delta W_i - W_{cu} \tag{4.132}$$

where W_i = force exerted by spreader at O_u and O_b before application of P
ΔW_i = change in spreader force due to P
W_{cu} = load at O_u from weight of upper cable
A_{Lu} = cross-sectional area of upper-cable segment on the left of O_u
l_{Lu} = length of chord from O_u to L_u
A_{Ru} = cross-sectional area of upper-cable segment on the right of O_u
l_{Ru} = length of chord from O_u to R_u

For joint O_b, Eq. (4.131*a*) becomes, on replacement of subscript u by b,

$$\frac{EA_{Lb}}{l_{Lb}} \cos^2 \alpha_{Lb}(\delta_L - \delta_O) + \frac{EA_{Rb}}{l_{Rb}} \cos^2 \alpha_{Rb}(\delta_R - \delta_O) = -P - W_i + \Delta W_i - W_{cb} \tag{4.133}$$

where W_{cb} is the load at O_b due to weight of lower cable and spreader.

Thus, for a cable truss with m joints in each cable, there are m unknown vertical displacements δ and m unknown changes in spreader force ΔW_i. Equations (4.132) and (4.133), applied to upper and lower nodes, respectively, provide $2m$ equations. Simultaneous solution of these equations yields the displacements and forces needed to complete the analysis.

The direction cosines in Eqs. (4.131) to (4.133), however, should be those for the displaced cable segments. If the direction cosines of the original geometry of a cable network are used in these equations, the computed deflections will be larger than the true deflections, because cables become stiffer as sag increases. The computed displacements, however, may be used to obtain revised direction cosines. The equations may then by solved again to yield corrected displacements. The process can be repeated as many times as necessary for convergence, as was shown for a single cable in Art 4.8.

For cable networks in general, convergence can often be speeded by computing the direction cosines for the third cycle of solution with node displacements that are obtained by averaging the displacements at each node computed in the first two cycles.

(H. Max Irvine, "*Cable Structures*", MIT Press, Cambridge, Mass.; Prem Krishna, *Cable-Suspended Roofs,* McGraw-Hill, Inc., New York; J. B. Scalzi et al., *Design Fundamentals of Cable Roof Structures,* U.S. Steel Corp., Pittsburgh, Pa.; J. Szabo and L. Kollar, *Structural Design of Cable-Suspended Roofs,* Ellis Horwood Limited, Chichester, England.)

4.11 PLANE-GRID FRAMEWORKS

A **plane grid** comprises a system of two or more members occurring in a single plane, interconnected at intersections, and carrying loads perpendicular to the plane. Grids comprised of beams, all occurring in a single plane, are referred to as **single-layer grids.** Grids comprised of trusses and those with bending members located in two planes with members maintaining a spacing between the planes are usually referred to as **double-layer grids.**

The connection between the grid members is such that all members framing into a particular joint will be forced to deflect the same amount. They are also connected so that bending moment is transferred across the joint. Although it is possible that torsion may be transferred into adjacent members, normally, torsion is not considered in grids comprised of steel beams because of their low torsional stiffness.

Methods of analyzing single- and double-layer framing generally are similar. This article therefore will illustrate the technique with the simpler plane framing and with girders instead of plane trusses. Loading will be taken as vertical. Girders will be assumed continuous at all nodes, except supports.

Girders may be arranged in numerous ways for plane-grid framing. Figure 4.19 shows some ways of placing two sets of girders. The grid in Fig. 4.19*a* consists of orthogonal sets laid perpendicular to boundary girders. Columns may be placed at the corners, along the boundaries, or at interior nodes. In the following analysis, for illustrative purposes, columns will be assumed only at the corners, and interior girders will be assumed simply supported on the boundary girders. With wider spacing of interior girders, the arrangement shown in Fig. 4.19*b* may be preferable. With beams in alternate bays spanning in perpendicular directions, loads are uniformly distributed to the girders. Alternatively, the interior girders may be set parallel to the main diagonals, as indicated in Fig. 4.19*c*. The method of analysis for this case is much the same as for girders perpendicular to boundary members. The structure, however, need not be rectangular or square, nor need the interior members be limited to two sets of girders.

Many methods have been used successfully to obtain exact or nearly exact solutions for grid framing, which may be highly indeterminate These include consistent deflections, finite differences, moment distribution or slope deflection, flat plate analogy, and model analysis. This article will be limited to illustrating the use of the method of consistent deflections.

In this method, each set of girders is temporarily separated from the other sets. Unknown loads satisfying equilibrium conditions then are applied to each set. Equations are obtained by expressing node deflections in terms of the loads and equating the deflection at each node of one set to the deflection of the same node in another set. Simultaneous solution of the equations yields the unknown loads on each set. With these now known, bending moments, shears, and deflections of all the girders can be computed by conventional methods.

For a simply supported grid, the unknowns generally can be selected and the equations formulated so that there is one unknown and one equation for each interior node. The number of equations required, however, can be drastically reduced if the framing is made symmetrical about perpendicular axes and the loading is symmetrical or antisymmetrical. For symmetrical grids subjected to unsymmetrical loading, the amount of work involved in analysis often can be decreased by resolving loads into symmetrical and antisymmetrical components. Figure 4.20 shows how this can be done for a single load unsymmetrically located on a grid. The analysis requires the solution of four sets of simultaneous equations and addition of the results, but there are fewer equations in each set than for unsymmetrical loading. The number of unknowns may be further decreased when the proportion of a load at a node to be assigned

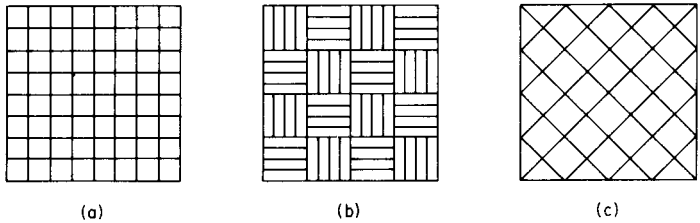

FIGURE 4.19 Orthogonal grids. (*a*) Girders on short spacing. (*b*) Girders on wide spacing with beams between them. (*c*) Girders set diagonally.

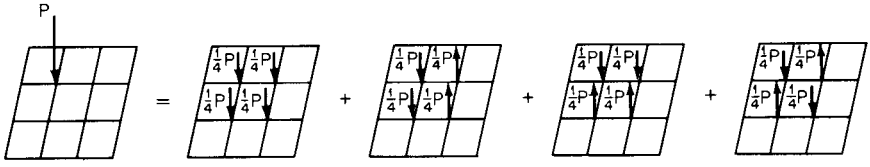

FIGURE 4.20 Resolution of a load into symmetrical and antisymmetrical components.

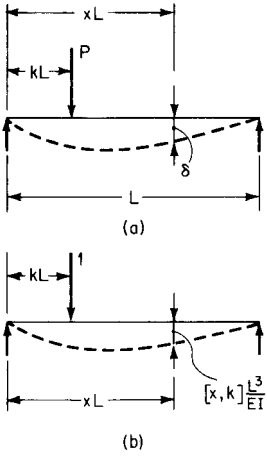

FIGURE 4.21 Single concentrated load on a beam. (*a*) Deflection curve. (*b*) Influence-coefficients curve for deflection at *xL* from support.

to a girder at that node can be determined by inspection or simple computation. For example, for a square orthogonal grid, each girder at the central node carries half the load there when the grid loading is symmetrical or antisymmetrical.

For analysis of simply supported grid girders, influence coefficients for deflection at any point induced by a unit load are useful. They may be computed from the following formulas.

The deflection at a distance *xL* from one support of a girder produced by a concentrated load *P* at a distance *kL* from that support (Fig. 4.21) is given by

$$\delta = \frac{PL^3}{6EI} x(1 - k)(2k - k^2 - x^2) \quad 0 \le x \le k \tag{4.134}$$

$$\delta = \frac{PL^3}{6EI} k(1 - x)(2x - x^2 - k^2) \quad k \le x \le 1 \tag{4.135}$$

where L = span of simply supported girder
E = modulus of elasticity of the steel
I = moment of inertia of girder cross section

The intersection of two sets of orthogonal girders produces a series of girders which may conveniently be divided into a discrete number of segments. The analysis of these girders will require the determination of deflections for each of these segments. The deflections that result from the application of Eqs. 4.134 and 4.135 to a girder divided into equal segments may be conveniently presented in table format as shown in Table 4.4 for girders divided into up to ten equal segments. The deflections can be found from the coefficients $C1$ and $C2$ as illustrated by the following example. Consider a beam of length L comprised of four equal segments ($N = 4$). If a load P is applied at $2L/N$ or $L/2$, the deflection at $1L/N$ or $L/4$ is

$$\frac{C2PL^3}{C1EI} = \frac{11}{768} \frac{PL^3}{EI}$$

For deflections, the elastic curve is also the influence curve, when $P = 1$. Hence the influence coefficient for any point of the girder may be written

TABLE 4.4 Deflection Coefficients for Beam of Length L Comprised of N Segments*

N	Defln. point, L/N	Coefficient $C2$ for load position, L/N									$C1$
		1	2	3	4	5	6	7	8	9	
2	1	1									48
3	1	8	7								486
	2	7	8								
4	1	9	11	7							768
	2	11	16	11							
	3	7	11	9							
5	1	32	45	40	23						3750
	2	45	72	68	40						
	3	40	68	72	45						
	4	23	40	45	32						
6	1	25	38	39	31	17					3888
	2	38	64	69	56	31					
	3	39	69	81	69	39					
	4	31	56	69	64	38					
	5	17	31	39	38	25					
7	1	72	115	128	117	88	47				14,406
	2	115	200	232	216	164	88				
	3	128	232	288	279	216	117				
	4	117	216	279	288	232	128				
	5	88	164	216	232	200	115				
	6	47	88	117	128	115	72				
8	1	49	81	95	94	81	59	31			12,288
	2	81	144	175	176	153	112	59			
	3	95	175	225	234	207	153	81			
	4	94	176	234	256	234	176	94			
	5	81	153	207	234	225	175	95			
	6	59	112	153	276	175	144	81			
	7	31	59	81	94	95	81	49			
9	1	128	217	264	275	256	213	152	79		39,366
	2	217	392	492	520	488	408	292	152		
	3	264	492	648	705	672	567	408	213		
	4	275	520	705	800	784	672	488	256		
	5	256	488	672	784	800	705	520	275		
	6	213	408	567	672	705	648	492	264		
	7	152	292	408	488	520	492	392	217		
	8	79	152	213	256	275	264	217	128		
10	1	81	140	175	189	185	166	135	95	49	30,000
	2	140	256	329	360	355	320	261	184	95	
	3	175	329	441	495	495	450	369	261	135	
	4	189	360	495	576	590	544	450	320	166	
	5	185	355	495	590	625	590	495	355	185	
	6	166	320	450	544	590	576	495	360	189	
	7	135	261	369	450	495	495	441	329	175	
	8	95	184	261	320	355	360	329	256	140	
	9	49	95	135	166	185	189	175	140	81	

* Deflection $= \dfrac{C2PL^3}{C1EI}$

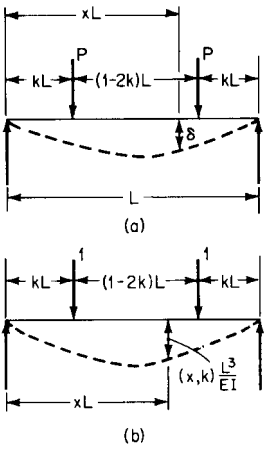

FIGURE 4.22 Two equal downward-acting loads symmetrically placed on a beam. (*a*) Deflection curve. (*b*) Influence-coefficients curve.

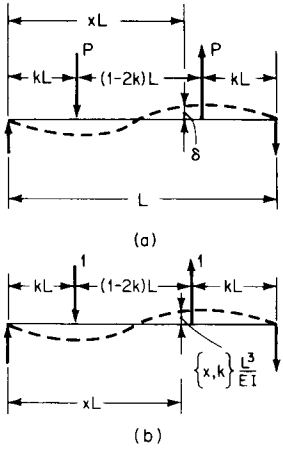

FIGURE 4.23 Equal upward and downward concentrated loads symmetrically placed on a beam. (*a*) Deflection curve. (*b*) Influence-coefficients curve.

$$\delta' = \frac{L^3}{EI}[x, k] \tag{4.136}$$

where

$$[x, k] = \begin{cases} \dfrac{x}{6}(1 - k)(2k - k^2 - x^2) & 0 \le x \le k \\ \dfrac{k}{6}(1 - x)(2x - x^2 - k^2) & k \le x \le 1 \end{cases} \tag{4.137}$$

The deflection at a distance xL from one support of the girder produced by concentrated loads P t distances kL and $(1 - k)L$ from that support Fig. 4.20) is given by

$$\delta = \frac{PL^3}{EI}(x, k) \tag{4.138}$$

where

$$(x, k) = \begin{cases} \dfrac{x}{6}(3k - 3k^2 - x^2) & 0 \le x \le k \\ \dfrac{k}{6}(3x - 3x^2 - k^2) & k \le x \le \dfrac{1}{2} \end{cases} \tag{4.139}$$

The deflection at a distance xL from one support of the girder produced by concentrated loads P at distance kL from the support and an upward concentrated load P at a distance $(1 - k)L$ from the support (antisymmetrical loading, Fig. 4.23) is given by

$$\delta = \frac{PL^3}{EI}\{x, k\} \tag{4.140}$$

where

$$[x, k] = \begin{cases} \dfrac{x}{6}(1 - 2k)(k - k^2 - x^2) & 0 \le x \le k \\ \dfrac{k}{6}(1 - 2x)(x - x^2 - k^2) & k \le x \le \dfrac{1}{2} \end{cases} \tag{4.141}$$

For convenience in analysis, the loading carried by the grid framing is converted into

concentrated loads at the nodes. Suppose for example that a grid consists of two sets of parallel girders as in Fig. 4.19, and the load at interior node r is P_r. Then it is convenient to assume that one girder at the node is subjected to an unknown force X_r there, and the other girder therefore carries a force $P_r - X_r$ at the node. With one set of girders detached from the other set, the deflections produced by these forces can be determined with the aid of Eqs. (4.134) to (4.141).

A simple example will be used to illustrate the application of the method of consistent deflections. Assume an orthogonal grid within a square boundary (Fig. 4.24*a*). There are $n = 4$ equal spaces of width h between girders. Columns are located at the corners A, B, C, and D. All girders have a span $nh = 4h$ and are simply supported at their terminals, though continuous at interior nodes. To simplify the example. all girders are assumed to have equal and constant moment of inertia I. Interior nodes carry a concentrated load P. Exterior nodes, except corners, are subjected to a load $P/2$.

Because of symmetry, only five different nodes need be considered. These are numbered from 1 to 5 in Fig. 4.24*a*, for identification. By inspection, loads P at nodes 1 and 3 can be distributed equally to the girders spanning in the x and y directions. Thus, when the two sets of parallel girders are considered separated, girder 4-4 in the x direction carries a load of $P/2$ at midspan (Fig. 4.24*b*). Similarly, girder 5-5 in the y direction carries loads of $P/2$ at the quarter points (Fig. 4.24*c*).

Let X_2 be the load acting on girder 4-4 (x direction) at node 2 (Fig. 4.24*b*). Then $P - X_2$ acts on girder 5-5 (y direction) at midspan (Fig. 4.24*c*). The reactions R of girders 4-4 and 5-5 are loads on the boundary girders (Fig. 4.24*d*).

Because of symmetry, X_2 is the only unknown in this example. Only one equation is needed to determine it.

To obtain this equation. equate the vertical displacement of girder 4-4 (x direction) at node 2 to the vertical displacement of girder 5-5 (y direction) at node 2. The displacement of girder 4-4 equals its deflection plus the deflection of node 4 on BC. Similarly, the displacement of girder 5-5 equals its deflection plus the deflection of node 5 on AB or its equivalent BC.

When use is made of Eqs. (4.136) and (4.138), the deflection of girder 4-4 (x direction) at node 2 equals

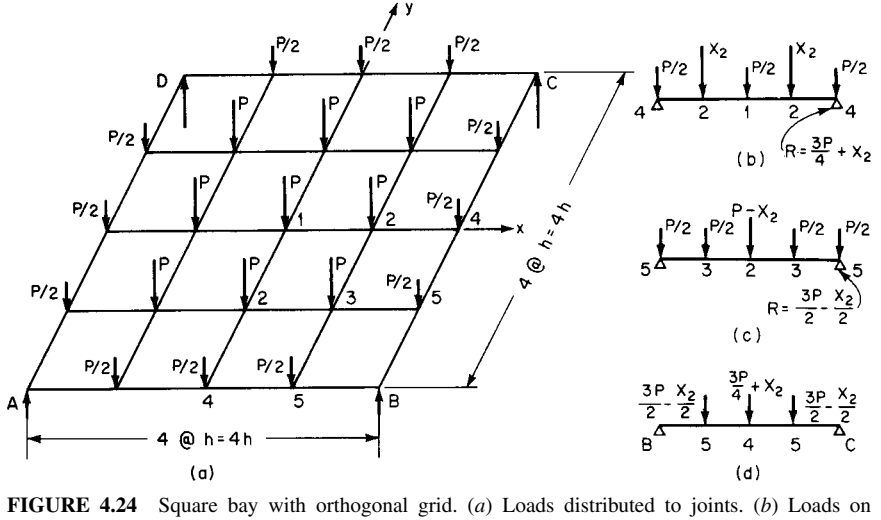

FIGURE 4.24 Square bay with orthogonal grid. (*a*) Loads distributed to joints. (*b*) Loads on midspan girder. (*c*) Loads on quarter-point girder. (*d*) Loads on boundary girder.

$$\delta_2 = \frac{n^3h^3}{EI}\left\{\left[\frac{1}{4}, \frac{1}{2}\right]\frac{P}{2} + \left(\frac{1}{4}, \frac{1}{4}\right)X_2\right\} + \delta_4 \tag{4.142a}$$

where δ_4 is the deflection of BC at node 4. By Eq. (4.137), [¼, ½] = (1⁄48)(11⁄16). By Eq. (4.139), (¼, ¼) = 1⁄48. Hence

$$\delta_2 = \frac{n^3h^3}{48EI}\left(\frac{11}{32}P + X_2\right) + \delta_4 \tag{4.142b}$$

For the loading shown in Fig. 4.24*d*,

$$\delta_4 = \frac{n^3h^3}{EI}\left\{\left[\frac{1}{2}, \frac{1}{2}\right]\left(\frac{3P}{4} + X_2\right) + \left(\frac{1}{2}, \frac{1}{4}\right)\left(\frac{3P}{2} - \frac{x_2}{2}\right)\right\} \tag{4.143a}$$

By Eq. (4.137), [½, ½] = 1⁄48. By Eq. (4.139), (½, ¼) = (1⁄48)(11⁄8). Hence Eq. (4.143*a*) becomes

$$\delta_4 = \frac{n^3h^3}{48EI}\left(\frac{45}{16}P + \frac{5}{16}X_2\right) \tag{4.143b}$$

Similarly, the deflection of girder 5-5 (y direction) at node 2 equals

$$\delta_2 = \frac{n^3h^3}{EI}\left\{\left[\frac{1}{2}, \frac{1}{2}\right](P - X_2) + \left(\frac{1}{2}, \frac{1}{4}\right)\frac{P}{2}\right\} + \delta_5 = \frac{n^3h^3}{48EI}\left(\frac{27}{16}P - X_2\right) + \delta_5 \tag{4.144}$$

For the loading shown in Fig. 4.24*d*,

$$\begin{aligned}\delta_5 &= \frac{n^3h^3}{EI}\left\{\left[\frac{1}{4}, \frac{1}{2}\right]\left(\frac{3P}{4} + X_2\right) + \left(\frac{1}{4}, \frac{1}{4}\right)\left(\frac{3P}{2} - \frac{X_2}{2}\right)\right\} \\ &= \frac{n^3h^3}{48EI}\left(\frac{129}{64}P + \frac{3}{16}X_2\right)\end{aligned} \tag{4.145}$$

The needed equation for determining X_2 is obtained by equating the right-hand side of Eqs. (4.142*b*) and (4.144) and substituting δ_4 and δ_5 given by Eqs. (4.143*b*) and (4.145). The result, after division of both sides of the equation by $n^3h^3/48EI$. is

$$^{11}\!/_{32}P + X_2 + {}^{45}\!/_{16}P + {}^{5}\!/_{16}X_2 = {}^{27}\!/_{16}P - X_2 + {}^{129}\!/_{64}P + {}^{3}\!/_{16}X_2 \tag{4.146}$$

Solution of the equation yields

$$X_2 = \frac{35P}{136} = 0.257P \qquad \text{and} \qquad P - X_2 = \frac{101P}{136} = 0.743P$$

With these forces known, the bending moments, shears, and deflections of the girders can be computed by conventional methods.

To examine a more general case of symmetrical framing, consider the orthogonal grid with rectangular boundaries in Fig. 4.25*a*. In the x direction, there are n spaces of width h. In the y direction, there are m spaces of width k. Only members symmetrically placed in the grid are the same size. Interior nodes carry a concentrated load P. Exterior nodes, except corners, carry $P/2$. Columns are located at the corners. For identification, nodes are numbered in one quadrant. Since the loading, as well as the framing, is symmetrical, corresponding nodes in the other quadrants may be given corresponding numbers.

At any interior node r, let X_r be the load carried by the girder spanning in the x direction. Then $P - X_r$ is the load at that node applied to the girder spanning in the y direction. For this example, therefore, there are six unknowns X_r, because r ranges from 1 to 6. Six equa-

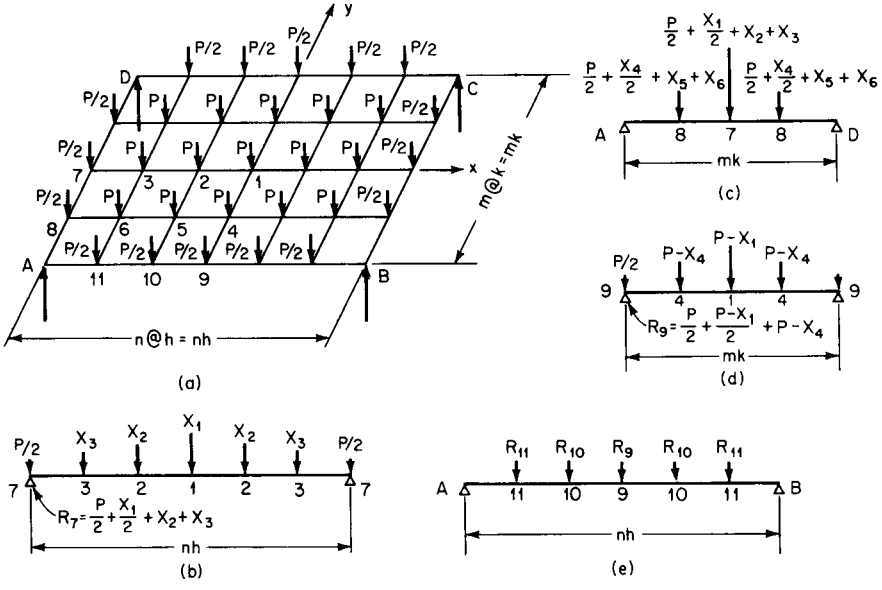

FIGURE 4.25 Rectangular bay with orthogonal girder grid. (*a*) Loads distributed to joints. (*b*) Loads on longer midspan girder. (*c*) Loads on shorter boundary girder *AD*. (*d*) Loads on shorter midspan girder. (*e*) Loads on longer boundary girder *AB*.

tions are needed for determination of X_r. They may be obtained by the method of consistent deflections. At each interior node, the vertical displacement of the *x*-direction girder is equated to the vertical displacement of the *y*-direction girder, as in the case of the square grid.

To indicate the procedure for obtaining these equations, the equation for node 1 in Fig. 4.25*a* will be developed. When use is made of Eqs. (4.136) and (4.138), the deflection of girder 7-7 at node 1 (Fig. 4.25*b*) equals

$$\delta_1 = \frac{n^3h^3}{EI_7}\left\{\left[\frac{1}{2}, \frac{1}{2}\right] X_1 + \left(\frac{1}{2}, \frac{1}{3}\right) X_2 + \left(\frac{1}{2}, \frac{1}{6}\right) X_3\right\} + \delta_7 \tag{4.147}$$

where I_7 = moment of inertia of girder 7-7
δ_7 = deflection of girder *AD* at node 7

Girder *AD* carries the reactions of the interior girders spanning in the *x* direction (Fig. 4.25*c*):

$$\delta_7 = \frac{m^3k^3}{EI_{AD}}\left\{\left[\frac{1}{2}, \frac{1}{2}\right]\left(\frac{P}{2} + \frac{X_1}{2} + X_2 + X_3\right) + \left(\frac{1}{2}, \frac{1}{4}\right)\left(\frac{P}{2} + \frac{X_4}{2} + X_5 + X_6\right)\right\} \tag{4.148}$$

where I_{AD} is the moment of inertia of girder *AD*. Similarly, the deflection of girder 9-9 at node 1 (Fig. 4.25*d*) equals

$$\delta_1 = \frac{m^3k^3}{EI_9}\left\{\left[\frac{2}{2}, \frac{1}{2}\right](P - X_1) + \left(\frac{1}{2}, \frac{1}{4}\right)(P - X_4)\right\} + \delta_9 \tag{4.149}$$

where I_9 = moment of inertia of girder 9-9
δ_9 = deflection of girder *AB* at node 9

Girder *AB* carries the reactions of the interior girders spanning in the *y* direction (Fig. 4.25*e*):

$$\delta_9 = \frac{n^3h^3}{EI_{AB}}\left\{\left[\frac{1}{2},\frac{1}{2}\right]\left(\frac{P}{2}+\frac{P-X_1}{2}+P-X_4\right)+\left(\frac{1}{2},\frac{1}{3}\right)\left(\frac{P}{2}+\frac{P-X_2}{2}+P-X_5\right)+\left(\frac{1}{2},\frac{1}{6}\right)\left(\frac{P}{2}+\frac{P-X_3}{2}+P-X_6\right)\right\} \tag{4.150}$$

where I_{AB} is the moment of inertia of girder *AB*. The equation for vertical displacement at node 1 is obtained by equating the right-hand side of Eqs. (4.147) and (4.149) and substituting δ_7 and δ_9 given by Eqs. (4.148) and (4.150).

After similar equations have been developed for the other five interior nodes, the six equations are solved simultaneously for the unknown forces X_r. When these have been determined, moments, shears, and deflections for the girders can be computed by conventional methods.

(A. W. Hendry and L. G. Jaeger, *Analysis of Grid Frameworks and Related Structures,* Prentice-Hall, Inc., Englewood Cliffs, N.J.; Z. S. Makowski, *Steel Space Structures,* Michael Joseph, London.)

4.12 FOLDED PLATES

Planar structural members inclined to each other and connected along their longitudinal edges comprise a **folded-plate structure** (Fig. 4.26). If the distance between supports in the longitudinal direction is considerably larger than that in the transverse direction, the structure acts much like a beam in the longitudinal direction. In general, however, conventional beam theory does not accurately predict the stresses and deflections of folded plates.

A folded-plate structure may be considered as a series of girders or trusses leaning against each other. At the outer sides, however, the plates have no other members to lean against. Hence the edges at boundaries and at other discontinuities should be reinforced with strong members to absorb the bending stresses there. At the supports also, strong members are needed to transmit stresses from the plates into the supports. The structure may be simply supported, or continuous, or may cantilever beyond the supports.

Another characteristic of folded plates that must be taken into account is the tendency of the inclined plates to spread. As with arches, provision must be made to resist this displacement. For the purpose, diaphragms or ties may be placed at supports and intermediate points.

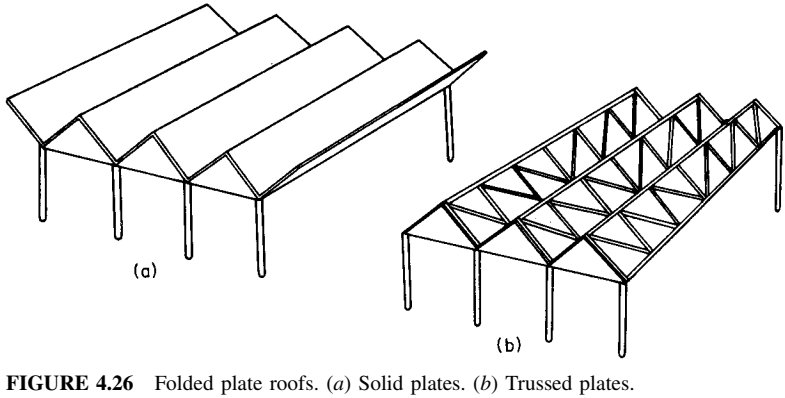

FIGURE 4.26 Folded plate roofs. (*a*) Solid plates. (*b*) Trussed plates.

The plates may be constructed in different ways. For example, each plate may be a stiffened steel sheet or hollow roof decking (Fig. 4.26*a*). Or it may be a plate girder with solid web. Or it may be a truss with sheet or roof decking to distribute loads transversely to the chords (Fig. 4.26*b*).

A folded-plate structure has a two-way action in transmitting loads to its supports. In the transverse direction, the plates act as slabs spanning between plates on either side. Each plate then serves as a girder in carrying the load received from the slabs longitudinally to the supports.

The method of analysis to be presented assumes the following: The material is elastic, isotropic, and homogeneous. Plates are simply supported but continuously connected to adjoining plates at fold lines. The longitudinal distribution of all loads on all plates is the same. The plates carry loads transversely only by bending normal to their planes and longitudinally only by bending within their planes. Longitudinal stresses vary linearly over the depth of each plate. Buckling is prevented by adjoining plates. Supporting members such as diaphragms, frames, and beams are infinitely stiff in their own planes and completely flexible normal to their planes. Plates have no torsional stiffness normal to their own planes. Displacements due to forces other than bending moments are negligible.

With these assumptions, the stresses in a steel folded-plate structure can be determined by developing and solving a set of simultaneous linear equations based on equilibrium conditions and compatibility at fold lines. The following method of analysis, however, eliminates the need for such equations.

Figure 4.27*a* shows a transverse section through part of a folded-plate structure. An interior element, plate 2, transmits the vertical loading on it to joints 1 and 2. Usual procedure is to design a 1-ft-wide strip of plate 2 at midspan to resist the transverse bending moment. (For continuous plates and cantilevers, a 1-ft-wide strip at supports also would be treated in the same way as the midspan strip.) If the load is w_2 kips per ft^2 on plate 2, the maximum

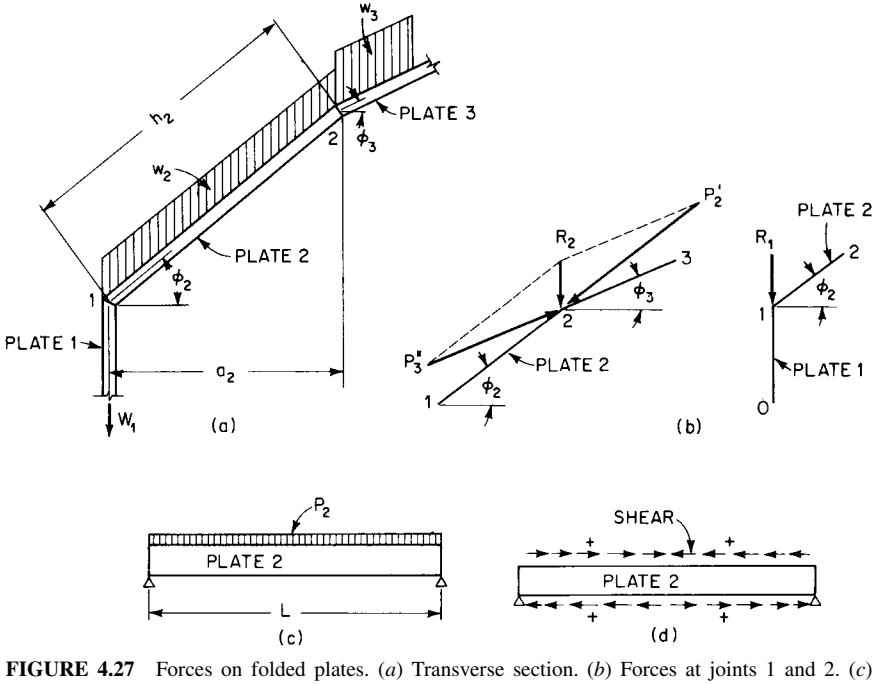

FIGURE 4.27 Forces on folded plates. (*a*) Transverse section. (*b*) Forces at joints 1 and 2. (*c*) Plate 2 acting as girder. (*d*) Shears on plate 2.

bending moment in the transverse strip is $w_2h_2a_2/8$, where h_2 is the depth (feet) of the plate and a_2 is the horizontal projection of h_2.

The 1-ft-wide transverse strip also must be capable of resisting the maximum shear $w_2h_2/2$ at joints 1 and 2. In addition, vertical reactions equal to the shear must be provided at the fold lines. Similarly, plate 1 applies a vertical reaction W_1 kips per ft at joint 1, and plate 3, a vertical reaction $w_3h_3/2$ at joint 2. Thus the total vertical force from the 1-ft-wide strip at joint 2 is

$$R_2 = \tfrac{1}{2}(w_2h_2 + w_3h_3) \tag{4.151}$$

Similar transverse strips also load the fold line. It may be considered subject to a uniformly distributed load R_2 kips per ft. The inclined plates 2 and 3 then carry this load in the longitudinal direction to the supports (Fig. 4.27*c*). Thus each plate is subjected to bending in its inclined plane.

The load to be carried by plate 2 in its plane is determined by resolving R_1 at joint 1 and R_2 at joint 2 into components parallel to the plates at each fold line (Fig. 4.27*b*). In the general case, the load (positive downward) of the nth plate is

$$P_n = \frac{R_n}{k_n \cos \phi_n} - \frac{R_{n-1}}{k_{n-1} \cos \phi_n} \tag{4.152}$$

where R_n = vertical load, kips per ft, on joint at top of plate n
R_{n-1} = vertical load, kips per ft, on joint at bottom of plate n
ϕ_n = angle, deg, plate n makes with the horizontal
k_n = $\tan \phi_n - \tan \phi_{n+1}$

This formula, however, cannot be used directly for plate 2 in Fig. 4.27(*a*) because plate 1 is vertical. Hence the vertical load at joint 1 is carried only by plate 1. So plate 2 must carry

$$P_2 = \frac{R_2}{k_2 \cos \phi_2} \tag{4.153}$$

To avoid the use of simultaneous equations for determining the bending stresses in plate 2 in the longitudinal direction, assume temporarily that the plate is disconnected from plates 1 and 3. In this case, maximum bending moment, at midspan, is

$$M_2 = \frac{P_2L^2}{8} \tag{4.154}$$

where L is the longitudinal span (ft). Maximum bending stresses then may be determined by the beam formula $f = \pm M/S$, where S is the section modulus. The positive sign indicates compression, and the negative sign tension.

For solid-web members, $S = I/c$, where I is the moment of inertia of the plate cross section and c is the distance from the neutral axis to the top or bottom of the plate. For trusses, the section modulus (in^3) with respect to the top and bottom, respectively, is given by

$$S_t = A_th \qquad S_b = A_bh \tag{4.155}$$

where A_t = cross-sectional area of top chord, in^2
A_b = cross-sectional area of bottom chord, in^2
h = depth of truss, in

In the general case of a folded-plate structure, the stress in plate n at joint n, computed on the assumption of a free edge, will not be equal to the stress in plate $n + 1$ at joint n,

similarly computed. Yet, if the two plates are connected along the fold line *n,* the stresses at the joint should be equal. To restore continuity, shears are applied to the longitudinal edges of the plates (Fig. 4.27*d*). The unbalanced stresses at each joint then may be adjusted by converging approximations, similar to moment distribution.

If the plates at a joint were of constant section throughout, the unbalanced stress could be distributed in proportion to the reciprocal of their areas. For a symmetrical girder, the unbalance should be distributed in proportion to the factor

$$F = \frac{1}{A}\left(\frac{h^2}{2r^2} + 1\right) \tag{4.156}$$

where A = cross-sectional area, in^2, of girder
h = depth, in, of girder
r = radius of gyration, in, of girder cross section

And for an unsymmetrical truss, the unbalanced stress at the top should be distributed in proportion to the factor

$$F_t = \frac{1}{A_t} + \frac{1}{A_b + A_t} \tag{4.157}$$

The unbalance at the bottom should be distributed in proportion to

$$F_b = \frac{1}{A_b} + \frac{1}{A_b + A_t} \tag{4.158}$$

A carry-over factor of $-\frac{1}{2}$ may be used for distribution to the adjoining edge of each plate. Thus the part of the unbalance assigned to one edge of a plate at a joint should be multiplied by $-\frac{1}{2}$, and the product should be added to the stress at the other edge.

After the bending stresses have been adjusted by distribution, if the shears are needed, they may be computed from

$$T_n = T_{n-1} - \frac{f_{n-1} + f_n}{2} A_n \tag{4.159}$$

for true plates, and for trusses, from

$$T_n = T_{n-1} - f_{n-1}A_b - f_nA_t \tag{4.160}$$

where T_n = shear, kips, at joint n
f_n = bending stress, ksi, at joint n
A_n = cross-sectional area, in^2, of plate n

Usually, at a boundary edge, joint 0, the shear is zero. With this known, the shear at joint 1 can be computed from the preceding equations. Similarly, the shear can be found at successive joints. For a simply supported, uniformly loaded, folded plate, the shear stress f_v (ksi) at any point on an edge n is approximately

$$f_v = \frac{T_{\max}}{18Lt}\left(\frac{1}{2} - \frac{x}{L}\right) \tag{4.161}$$

where x = distance, ft, from a support
t = web thickness of plate, in
L = longitudinal span, ft, of plate

As an illustration of the method, stresses will be computed for the folded-plate structure

in Fig. 28*a*. It may be considered to consist of four inverted-V girders, each simply supported with a span of 120 ft. The plates are inclined at an angle of 45° with the horizontal. With a rise of 10 ft and horizontal projection $a = 10$ ft, each plate has a depth $h = 14.14$ ft. The structure is subjected to a uniform load $w = 0.0353$ ksf over its surface. The inclined plates will be designed as trusses. The boundaries, however, will be reinforced with a vertical member, plate 1. The structure is symmetrical about joint 5.

As indicated in Fig. 28*a*, 1-ft-wide strip is selected transversely across the structure at midspan. This strip is designed to transmit the uniform load w to the folds. It requires a vertical reaction of $0.0353 \times 14.14/2 = 0.25$ kip per ft along each joint (Fig. 28*b*). Because of symmetry, a typical joint then is subjected to a uniform load of $2 \times 0.25 = 0.5$ kip per

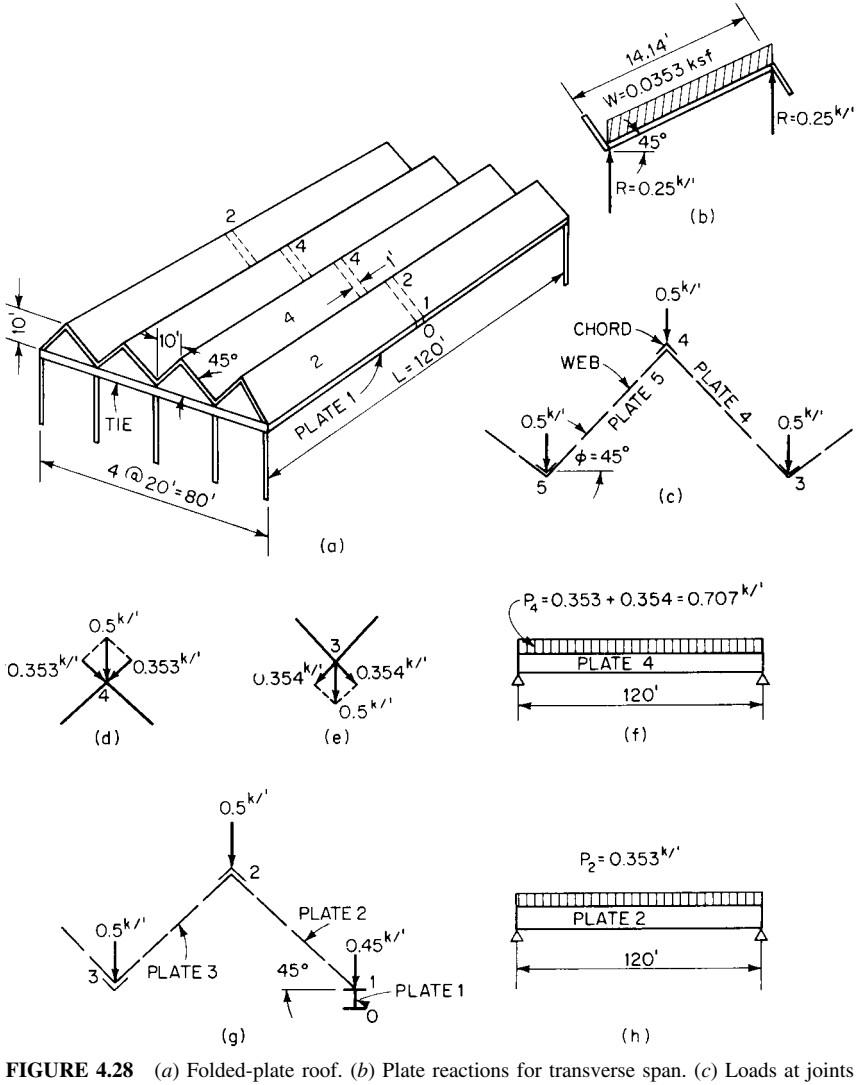

FIGURE 4.28 (*a*) Folded-plate roof. (*b*) Plate reactions for transverse span. (*c*) Loads at joints of typical interior transverse section. (*d*) Forces at joint 4. (*e*) Forces at joint 3. (*f*) Plate 4 acting as girder. (*g*) Loads at joints of outer transverse section. (*h*) Plate 2 acting as girder.

ft (Fig. 28*c*). At joint 1, the top of the vertical plate, however, the uniform load is 0.25 plus a load of 0.20 on plate 1, or 0.45 kip per ft (Fig. 28*g*).

The analysis may be broken into two parts, to take advantage of simplification permitted by symmetry. First. the stresses may be determined for a typical interior inverted-V girder. Then. the stresses may be computed for the boundary girders, including plate 1.

The typical interior girder consists of plates 4 and 5, with load of 0.5 kip per ft at joints 3, 4, and 5 (Fig. 28*c*). This load may be resolved into loads in the plane of the plates, as indicated in Fig. 28*d* and *e*. Thus a typical plate, say plate 4, is subjected to a uniform load of 0.707 kip per ft (Fig. 28*f*). Hence the maximum bending moment in this truss is

$$M = \frac{0.707(120)^2}{8} = 1273 \text{ ft-kips}$$

Assume now that each chord is an angle $8 \times 8 \times \frac{9}{16}$ in, with an area of 8.68 in^2. Then the chords, as part of plate 4, have a maximum bending stress of

$$f = \pm\frac{1273}{8.68 \times 14.14} = \pm 10.36 \text{ ksi}$$

Since the plate is typical, adjoining plates also impose an equal stress on the same chords. Hence the total stress in a typical chord is $\pm 10.36 \times 2 = \pm 20.72$ ksi, the stress being compressive along ridges and tensile along valleys.

To prevent the plates composing the inverted-V girder from spreading, a tie is needed at each support. This tie is subjected to a tensile force

$$P = R \cos \phi = 0.707(120/2)0.707 = 30 \text{ kips}$$

The boundary inverted-V girder consists of plates 1, 2, and 3, with a vertical load of 0.5 kip per ft at joints 2 and 3 and 0.45 kip per ft on joint 1. Assume that plate 1 is a W36 $\times$ 135. The following properties of this shape are needed: $A = 39.7$ in^2. $h = 35.55$ in. $A_f = 9.44$ in^2, $r = 14$ in, $S = 439$ in^3. Assume also that the top flange of plate 1 serves as the bottom chord of plate 2. Thus this chord has an area of 9.44 in^2.

With plate 1 vertical, the load on joint 1 is carried only by plate 1. Hence, as indicated by the resolution of forces in Fig. 28*d*, plate 2 carries a load in its plane of 0.353 kip per ft (Fig. 28*h*). The maximum bending moment due to this load is

$$M = \frac{0.353(120)^2}{8} = 637 \text{ ft-kips}$$

Assume now that the plates are disconnected along their edges. Then the maximum bending stress in the top chord of plate 2, including the stress imposed by bending of plate 3, is

$$f_t = \frac{637}{8.68 \times 14.14} + 10.36 = 5.18 + 10.36 = 15.54 \text{ ksi}$$

and the maximum stress in the bottom chord is

$$f_b = \frac{-637}{9.44 \times 14.14} = -4.77 \text{ ksi}$$

For the load of 0.45 kip per ft, plate 1 has a maximum bending moment of

$$M = \frac{0.45(120)^2 12}{8} = 9730 \text{ in-kips}$$

The maximum stresses due to this load are

$$f = \frac{M}{S} = \pm\frac{9730}{439} = \pm 22.16 \text{ ksi}$$

Because the top flange of the girder has a compressive stress of 22.16 ksi, whereas acting as the bottom chord of the truss, the flange has a tensile stress of 4.77 ksi, the stresses at joint 1 must be adjusted. The unbalance is 22.16 + 4.77 = 26.93 ksi;

The distribution factor at joint 1 for plate 2 can be computed from Eq. (4.158):

$$F_2 = \frac{1}{9.44} + \frac{1}{9.44 + 8.68} = 0.1611$$

The distribution factor for plate 1 can be obtained from Eq. (4.156):

$$F_1 = \frac{1}{39.7}\left[\frac{(35.5)^2}{2(14)^2} + 1\right] = 0.1062$$

Hence the adjustment in the stress in the girder top flange is

$$\frac{-26.93 \times 0.1062}{0.1062 + 0.1611} = -10.70 \text{ ksi}$$

The adjusted stress in that flange then is 22.16 − 10.70 = 11.46 ksi. The carryover to the bottom flange is (−½)(−10.70) = 5.35 ksi. And the adjusted bottom flange stress is −22.16 + 5.35 = −16.87 ksi.

Plate 2 receives an adjustment of 26.93 − 10.70 = 16.23 ksi. As a check, its adjusted stress is −4.77 + 16.23 = 11.46 ksi, the same as that in the top flange of plate 1. The carryover to the top chord is (−½)16.23 = −8.12. The unbalanced stress now present at joint 2 may be distributed in a similar manner, the distributed stresses may be carried over to joints 1 and 3, and the unbalance at those joints may be further distributed. The adjustments beyond joint 2, however, will be small.

(V. S. Kelkar and R. T. Sewell, *Fundamentals of the Analysis and Design of Shell Structures,* Prentice-Hall, Englewood Cliffs, N.J.)

4.13 ORTHOTROPIC PLATES

Plate equations are applicable to steel plate used as a deck. Between reinforcements and supports, a constant-thickness deck, loaded within the elastic range, acts as an isotropic elastic plate. But when a deck is attached to reinforcing ribs or is continuous over relatively closely spaced supports its properties change in those directions. The plate becomes **anistropic**. And if the ribs and floorbeams are perpendicular to each other, the plate is **orthogonal-anistropic,** or **orthotropic** for short.

An orthotropic-plate deck, such as the type used in bridges. resembles a plane-grid framework (Art. 4.11). But because the plate is part of the grid. an orthotropic-plate structure is even more complicated to analyze. In a bridge, the steel deck plate, protected against traffic and weathering by a wearing surface, serves as the top flange of transverse floorbeams and longitudinal girders and is reinforced longitudinally by ribs (Fig. 4.29). The combination of deck with beams and girders permits design of bridges with attractive long, shallow spans.

Ribs, usually of constant dimensions and closely spaced, are generally continuous at floorbeams. The transverse beams, however, may be simply supported at girders. The beams may be uniformly spaced at distances ranging from about 4 to 20 ft. Rib spacing ranges from 12 to 24 in.

Ribs may be either open (Fig. 4.30*a*) or closed (Fig. 4.30*b*). Open ribs are easier to fabricate and field splice. The underside of the deck is readily accessible for inspection and

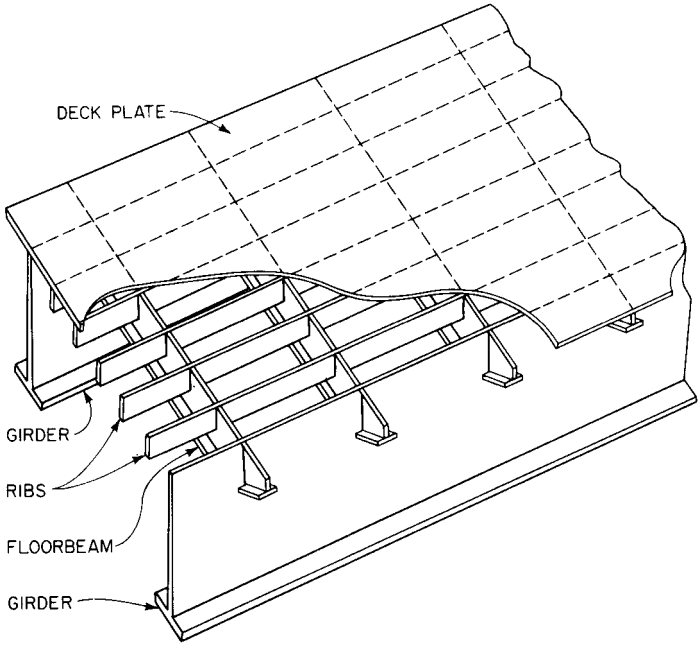

FIGURE 4.29 Orthotropic plate.

maintenance. Closed ribs, however, offer greater resistance to torsion. Load distribution consequently is more favorable. Also, less steel and less welding are required than for open-rib decks.

Because of the difference in torsional rigidity and load distribution with open and closed ribs, different equations are used for analyzing the two types of decks. But the general procedure is the same for both.

Stresses in an orthotropic plate are assumed to result from bending of four types of members:

Member I comprises the plate supported by the ribs (Fig. 4.31*a*). Loads between the ribs cause the plate to bend.

Member II consists of plate and longitudinal ribs. The ribs span between and are continuous at floorbeams (Fig. 4.31*b*). Orthotropic analysis furnishes distribution of loads to ribs and stresses in the member.

Member III consists of the reinforced plate and the transverse floorbeams spanning between girders (Fig. 4.31*c*). Orthotropic analysis gives stresses in beams and plate.

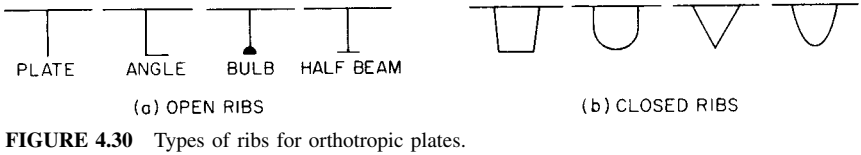

FIGURE 4.30 Types of ribs for orthotropic plates.

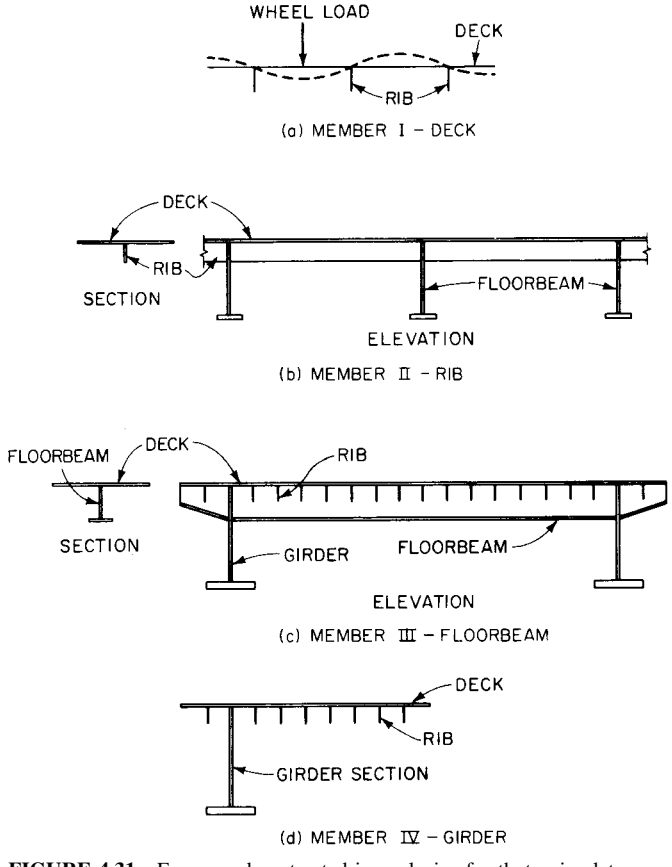

FIGURE 4.31 Four members treated in analysis of orthotropic plates.

Member IV comprises girders and plate (Fig. 4.31*d*). Stresses are computed by conventional methods. Hence determination of girder and plate stresses for this member will not be discussed in this article.

The plate theoretically should be designed for the maximum principal stresses that result from superposition of all bending stresses. In practice, however, this is not done because of the low probability of the maximum stress and the great reserve strength of the deck as a membrane (second-order stresses) and in the inelastic range.

Special attention, however, should be given to stability against buckling. Also, loading should take into account conditions that may exist at intermediate erection stages.

Despite many simplifying assumptions, orthotropic-plate theories that are available and reasonably in accord with experiments and observations of existing structures require long, tedious computations. (Some or all of the work, however, may be done with computers to speed up the analysis.) The following method, known as the **Pelikan-Esslinger method,** has been used in design of several orthotropic plate bridges. Though complicated, it still is only an approximate method. Consequently, several variations of it also have been used.

In one variation, members II and III are analyzed in two stages. For the first stage, the floorbeams are assumed as rigid supports for the continuous ribs. Dead- and live-load shears,

reactions, and bending moments in ribs and floorbeams then are computed for this condition. For the second stage, the changes in live-load shears, reactions, and bending moments are determined with the assumption that the floorbeams provide elastic support.

Analysis of Member I. Plate thickness generally is determined by a thickness criterion. If the allowable live-load deflection for the span between ribs is limited to 1/300th of the rib spacing, and if the maximum deflection is assumed as one-sixth of the calculated deflection of a simply supported, uniformly loaded plate, the thickness (in) should be at least

$$t = 0.065a\sqrt[3]{p} \tag{4.162}$$

where a = spacing, in, of ribs
p = load, ksi

The calculated thickness may be increased, perhaps 1/16 in, to allow for possible metal loss due to corrosion.

The ultimate bearing capacity of plates used in bridge decks may be checked with a formula proposed by K. Kloeppel:

$$p_u = \frac{6.1 f_u t}{a}\sqrt{\epsilon_u} \tag{4.163}$$

where p_u = loading, ksi, at ultimate strength
ϵ_u = elongation of the steel, in per in, under stress f_u
f_u = ultimate tensile strength, ksi, of the steel
t = plate thickness, in

Open-Rib Deck-Member II, First Stage. Resistance of the orthotropic plate between the girders to bending in the transverse, or x, direction and torsion is relatively small when open ribs are used compared with flexural resistance in the y direction (Fig. 4.32*a*). A good approximation of the deflection w (in) at any point (x, y) may therefore be obtained by assuming the flexural rigidity in the x direction and torsional rigidity to be zero. In this case, w may be determined from

$$D_y \frac{\partial^4 w}{\partial y^4} = p(x, y) \tag{4.164}$$

where D_y = flexural rigidity of orthotropic plate in longitudinal, or y, direction, in-kips
$p(x, y)$ = load expressed as function of coordinates x and y, ksi

For determination of flexural rigidity of the deck, the rigidity of ribs is assumed to be continuously distributed throughout the deck. Hence the flexural rigidity in the y direction is

$$D_y = \frac{EI_r}{a} \tag{4.165}$$

where E = modulus of elasticity of steel, ksi
I_r = moment of inertia of one rib and effective portion of plate, in^4
a = rib spacing, in

Equation (4.164) is analogous to the deflection equation for a beam. Thus strips of the plate extending in the y direction may be analyzed with beam formulas with acceptable accuracy.

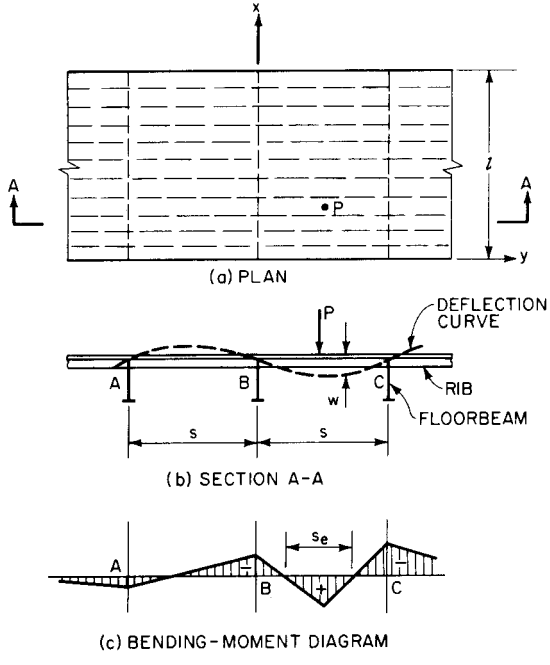

FIGURE 4.32 (*a*) For orthotropic-plate analysis, the x axis lies along a floorbeam, the y axis along a girder. (*b*) A rib deflects like a continuous beam. (*c*) Length of positive region of rib bending-moment diagram determines effective rib span s_e.

In the first stage of the analysis, bending moments are determined for one rib and the effective portion of the plate as a continuous beam on rigid supports. (In this and other phases of the analysis, influence lines or coefficients are useful. See, for example, Table 4.5 and Fig. 4.33.) Distribution of live load to the rib is based on the assumption that the ribs act as rigid supports for the plate. For a distributed load with width B in, centered over the rib, the load carried by the rib is given in Table 4.6 for B/a ranging from 0 to 3. For B/a from 3 to 4, the table gives the load taken by one rib when the load is centered between two ribs. The value tabulated in this range is slightly larger than that for the load centered over a rib. Uniform dead load may be distributed equally to all the ribs.

The effective width of plate as the top flange of the rib is a function of the rib span and end restraints. In a loaded rib, the end moments cause two inflection points to form. In computation of the effective width, therefore, the effective span s_e (in) of the rib should be taken as the distance between those points, or length of positive-moment region of the bending-moment diagram (Fig. 4.32*c*). A good approximation is

$$s_e = 0.7s \tag{4.166}$$

where s is the floorbeam spacing (in).

The ratio of effective plate width a_0 (in) to rib spacing a (in) is given in Table 4.6 for a range of values of B/a and a/s_e. Multiplication of a_0/a by a gives the width of the top flange of the T-shaped rib (Fig. 4.34).

TABLE 4.5 Influence Coefficients for Continuous Beam on Rigid Supports

Constant moment of inertia and equal spans

y/s	Midspan moments at C m_C/s	End moments at 0 m_0/s	Reactions at 0 r_0
0	0	0	1.000
0.1	0.0215	−0.0417	0.979
0.2	0.0493	−0.0683	0.922
0.3	0.0835	−0.0819	0.835
0.4	0.1239	−0.0849	0.725
0.5	0.1707	−0.0793	0.601
0.6	0.1239	−0.0673	0.468
0.7	0.0835	−0.0512	0.334
0.8	0.0493	−0.0331	0.207
0.9	0.0215	−0.0153	0.093
1.0	0	0	0
1.2	−0.0250	0.0183	−0.110
1.4	−0.0311	0.0228	−0.137
1.6	−0.0247	0.0180	−0.108
1.8	−0.0122	0.0089	−0.053
2.0	0	0	0
2.2	0.0067	−0.0049	0.029
2.4	0.0083	−0.0061	0.037
2.6	0.0066	−0.0048	0.029
2.8	0.0032	−0.0023	0.014
3.0	0	0	0

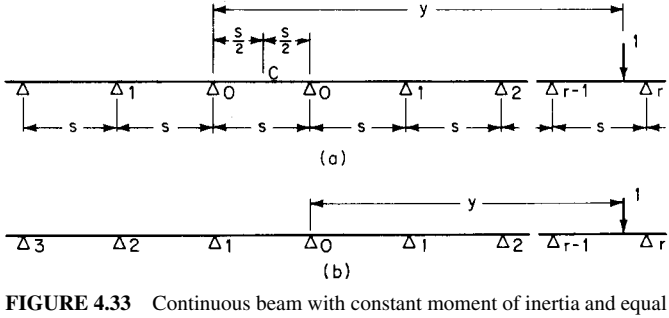

FIGURE 4.33 Continuous beam with constant moment of inertia and equal spans on rigid supports. (*a*) Coordinate y for load location for midspan moment at C. (*b*) Coordinate y for reaction and end moment at O.

TABLE 4.6 Analysis Ratios for Open Ribs

Ratio of load width to rib spacing B/a	Ratio of load on one rib to total load R_o/P	Ratio of effective plate width to rib spacing a_o/a for the following ratios of rib spacing to effective rib span a/s_e							
		0	0.1	0.2	0.3	0.4	0.5	0.6	0.7
0	1.000	2.20	2.03	1.62	1.24	0.964			
0.5	0.959	2.16	1.98	1.61	1.24	0.970	0.777		
1.0	0.854	2.03	1.88	1.56	1.24	0.956	0.776		
1.5	0.714	1.83	1.73	1.47	1.19	0.938	0.776		
2.0	0.567	1.60	1.52	1.34	1.12	0.922	0.760	0.641	
2.5	0.440	1.34	1.30	1.18	1.04	0.877	0.749	0.636	0.550
3.0	0.354	1.15	1.13	0.950	0.936	0.827	0.722	0.626	0.543
3.5	0.296	0.963	0.951	0.902	0.832	0.762	0.675	0.604	0.535
4.0	0.253	0.853	0.843	0.812	0.760	0.699	0.637	0.577	0.527

Open-Rib Deck-Member III, First Stage. For the condition of floorbeams acting as rigid supports for the rib, dead-load and live-load moments for a beam are computed with the assumption that the girders provide rigid support. The effective width s_o (in) of the plate acting as the top flange of the T-shaped floorbeam is a function of the span and end restraints. For a simply supported beam, in the computation of effective plate width, the effective span l_e (in) may be taken approximately as

$$l_e = l \tag{4.167}$$

where l is the floorbeam span (in).

For determination of floorbeam shears, reactions, and moments, s_o may be taken as the floorbeam spacing. For stress computations, the ratio of effective plate width s_o to effective beam spacing s_f (in) may be obtained from Table 4.7. When all beams are equally loaded

$$s_f = s \tag{4.168}$$

The effect of using this relationship for calculating stresses in unequally loaded floorbeams generally is small. Multiplication of s_o/s_f given by Table 4.7 by s yields, for practical purposes, the width of the top flange of the T-shaped floorbeam.

Open-Rib Deck-Member II, Second Stage. In the second stage, the floorbeams act as elastic supports for the ribs under live loads. Deflection of the beams, in proportion to the load they are subjected to, relieves end moments in the ribs but increases midspan moments.

Evaluation of these changes in moments may be made easier by replacing the actual live loads with equivalent sinusoidal loads. This permits use of a single mathematical equation

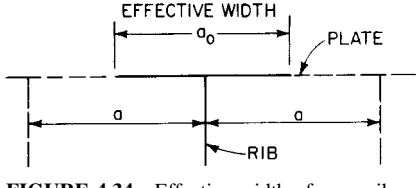

FIGURE 4.34 Effective width of open rib.

TABLE 4.7 Effective Width of Plate

a_e/s_e e_e/s_e s_f/l_e	a_o/a_e e_o/e_e s_o/s_f	a_e/s_e e_e/s_e s_f/l_e	a_o/a_e e_o/e_e s_o/s_f	a_e/s_e e_e/s_e s_f/l_e	a_o/a_e e_o/e_e s_o/s_f	a_e/s_e e_e/s_e s_f/l_e	a_o/a_e e_o/e_e s_o/s_f
0	1.10	0.20	1.01	0.40	0.809	0.60	0.622
0.05	1.09	0.25	0.961	0.45	0.757	0.65	0.590
0.10	1.08	0.30	0.921	0.50	0.722	0.70	0.540
0.15	1.05	0.35	0.870	0.55	0.671	0.75	0.512

for the deflection curve over the entire floorbeam span. For this purpose, the equivalent loading may be expressed as a Fourier series. Thus, for the coordinate system shown in Fig. 4.32*a*, a wheel load P kips distributed over a deck width B (in) may be represented by the Fourier series

$$Q_{nx} = \sum_{n=1}^{\infty} Q_n \sin \frac{n\pi x}{l} \tag{4.169}$$

where n = integer
x = distance, in, from support
l = span, in, or distance, in, over which equivalent load is distributed

For symmetrical loading, only odd numbers need be used for n. For practical purposes, Q_n may be taken as

$$Q_n = \frac{2P}{l} \sin \frac{n\pi x_P}{l} \tag{4.170}$$

where x_P is the distance (in) of P from the girder.

Thus, for two equal loads P centered over x_P and c in apart,

$$Q_n = \frac{4P}{l} \sin \frac{n\pi x_P}{l} \cos \frac{n\pi c}{2l} \tag{4.171}$$

For m pairs of such loads centered, respectively, over $x_1, x_2, \ldots, x_m$,

$$Q_n = \frac{4P}{l} \cos \frac{n\pi c}{2l} \sum_{r=1}^{m} \sin \frac{n\pi x_r}{l} \tag{4.172}$$

For a load W distributed over a lane width B (in) and centered over x_W,

$$Q_n = \frac{4W}{n\pi} \sin \frac{n\pi x_W}{l} \sin \frac{n\pi B}{2l} \tag{4.173}$$

And for a load W distributed over the whole span,

$$Q_n = \frac{4W}{n\pi l} \tag{4.174}$$

Bending moments and reactions for the ribs on elastic supports may be conveniently evaluated with influence coefficients. Table 4.8 lists such coefficients for midspan moment, end moment, and reaction of a rib for a unit load over any support (Fig. 4.35).

TABLE 4.8 Influence Coefficients for Continuous Beam on Elastic Supports
Constant moment of inertia and equal spans

Flexibility coefficient	Midspan moments m_C/s, for unit load at support:			End moments m_0/s, for unit load at support:				Reactions r_0, for unit load at support:		
γ	0	1	2	0	1	2	3	0	1	2
0.05	0.027	−0.026	−0.002	0.100	−0.045	−0.006	0.001	0.758	0.146	−0.034
0.10	0.045	−0.037	−0.010	0.142	−0.053	−0.021	0.001	0.611	0.226	−0.010
0.50	0.115	−0.049	−0.049	0.260	−0.031	−0.066	−0.032	0.418	0.256	0.069
1.00	0.161	−0.040	−0.069	0.323	−0.001	−0.079	−0.059	0.353	0.245	0.098
1.50	0.193	−0.029	−0.079	0.363	0.023	−0.082	−0.076	0.319	0.236	0.111
2.00	0.219	−0.019	−0.083	0.395	0.043	−0.181	−0.087	0.297	0.228	0.118
4.00	0.291	0.019	−0.087	0.479	0.104	−0.066	−0.108	0.250	0.206	0.127
6.00	0.341	0.049	−0.081	0.534	0.147	−0.048	−0.115	0.226	0.192	0.128
8.00	0.379	0.076	−0.073	0.577	0.182	−0.031	−0.115	0.210	0.182	0.128
10.00	0.411	0.098	−0.064	0.612	0.211	−0.015	−0.113	0.199	0.175	0.127

The influence coefficients are given as a function of the flexibility coefficient of the floorbeam:

$$\gamma = \frac{l^4 I_r}{\pi^4 s^3 a I_f} \tag{4.175}$$

where I_r = moment of inertia, in, of rib, including effective width of plate
I_f = moment of inertia, in, of floorbeam, including effective width of plate
s = rib span, in
a = rib spacing, in

For calculation of change in moment in the rib, use of only the first term of the series for the equivalent load Q_{1x} yields sufficiently accurate results in calculating the change in moments due to elasticity of the floorbeams. The increase in moment at midspan of a rib may be computed from

$$\Delta M_C = Q_{1x} sa \sum \frac{r_m m_{Cm}}{s} \tag{4.176}$$

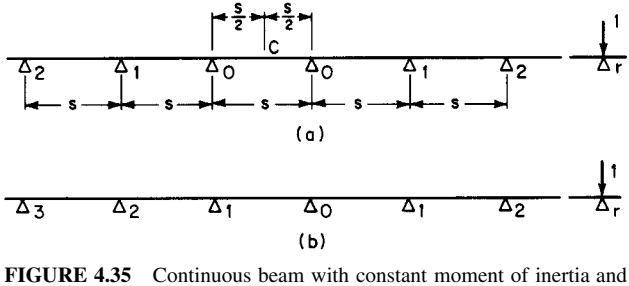

FIGURE 4.35 Continuous beam with constant moment of inertia and equal spans on elastic supports. Load over support for (*a*) midspan moment at *C*, and (*b*) reaction and support moment at *O*.

where r_m = influence coefficient for reaction of rib at support m when floorbeam provides rigid support
m_{Cm} = influence coefficient for midspan moment at C for load at support m when floorbeams provide elastic support

The summation in Eq. (4.176) is with respect to subscript m; that is, the effects of reactions at all floorbeams are to be added. The decrease in end moment in the rib may be similarly computed.

The effective width a_o of the rib in this stage may be taken as $1.10a$.

Open-Rib Deck-Member III, Second Stage. Deflection of a floorbeam reduces the reactions of the ribs there. As a result, bending moments also are decreased. The more flexible the floorbeams, the longer the portion of deck over which the loads are distributed and the greater the decrease in beam moment.

The decrease may be computed from

$$\Delta M_f = Q_{1x} \left(\frac{l}{\pi}\right)^2 \left(r_0 - \sum r_m r_{0m}\right) \tag{4.177}$$

where r_0 = influence coefficient for reaction of rib at support 0 (floorbeam for which moment reduction is being computed) when beam provides rigid support
r_m = influence coefficient for reaction of rib at support m when floorbeam provides rigid support
r_{0m} = influence coefficient for reaction of rib at support 0 for load over support m when floorbeams provide elastic support

The summation of Eq. (4.177) is with respect to m; that is, the effects of reactions at all floorbeams are to be added.

For computation of shears, reactions, and moments, the effective width of plate as the top flange of the floorbeam may be taken as the beam spacing s. For calculation of stresses, the effective width s_o may be obtained from Table 4.7 with $s_f = s$.

Open-Rib Deck-Member IV. The girders are analyzed by conventional methods. The effective width of plate as the top flange on one side of each girder may be taken as half the distance between girders on that side.

Closed-Rib Deck-Member II, First Stage. Resistance of closed ribs to torsion generally is large enough that it is advisable not to ignore torsion. Flexural rigidity in the transverse, or x, direction (Fig. 4.32*a*) may be considered negligible compared with torsional rigidity and flexural rigidity in the y direction. A good approximation of the deflection w (in) may therefore be obtained by assuming the flexural rigidity in the x direction to be zero. In that case, w may be determined from

$$D_y \frac{\partial^4 w}{\partial y^4} + 2H \frac{\partial w^4}{\partial x^2\, \partial y^2} = p(x, y) \tag{4.178}$$

where D_y = flexural rigidity of the orthotropic plate in longitudinal, or y, direction, in-kips
H = torsional rigidity of orthotropic plate, in-kips
$p(x, y)$ = load expressed as function of coordinates x and y, ksi

In the computation of D_y and H, the contribution of the plate to these parameters must be included. For the purpose, the effective width of plate acting as the top flange of a rib is obtained as the sum of two components. One is related to the width a (in) of the rib at the plate. The second is related to the distance e (in) between ribs (Fig. 4.36). These components may be computed with the aid of Table 4.7. For use with this table, the effective rib span

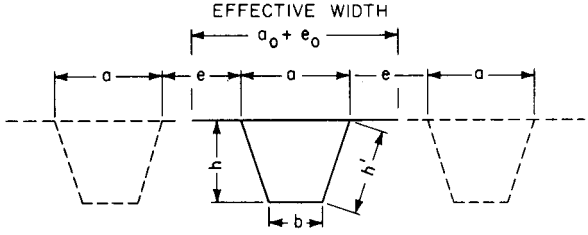

FIGURE 4.36 Effective width of a closed rib.

s_e (in) may be found from Eq. (4.166). For determination of shears, reactions, and moments, it is sufficiently accurate to take $a_e = a$ and $e_e = e$. (The error in using the resulting section for stress computations usually also will be small.) Then, in terms of the values given by Table 4.7, the effective plate width for a closed rib is

$$a'_o + e'_o = \frac{a_o}{a_e} a_e + \frac{e_o}{e_e} e_e \tag{4.179}$$

The flexural rigidity in the longitudinal direction usually is taken as the average for the orthotropic plate. Thus

$$D_y = \frac{EI_r}{a + e} \tag{4.180}$$

where E = modulus of elasticity of steel, ksi
I_r = moment of inertia, in^4, of rib, including effective plate width

Because of the flexibility of the orthotropic plate in the transverse direction, the full cross section is not completely effective in resisting torsion. Hence the formula for computing H includes a reduction factor v:

$$H = \frac{1}{2} \frac{vGK}{a + e} \tag{4.181}$$

where G = shearing modulus of elasticity of steel = 11,200 ksi
K = torsional factor, a function of the cross section

In general, for hollow closed ribs, the torsional factor may be determined from

$$K = \frac{4A_r^2}{p_e/t_r + a/t_p} \tag{4.182}$$

where A_r = mean of area enclosed by inner and outer boundaries of rib, in^2
p_e = perimeter of rib, exclusive of top flange, in
t_r = rib thickness, in
t_p = plate thickness, in

For a trapezoidal rib, for example,

$$K = \frac{(a + b)^2 h^2}{(b + 2h')/t_r + a/t_p} \tag{4.183}$$

where b = width, in, of rib base
h = depth, in, of rib
h' = length, in, of rib side

The reduction factor v may be determined analytically. The resulting formulas however, are lengthy, and their applicability to a specific construction is questionable. For a major structure, it is advisable to verify the torsional rigidity, and perhaps also the flexural rigidities, by model tests. For a trapezoidal rib, the reduction factor may be closely approximated by

$$\frac{1}{v} = 1 + \frac{GK}{EI_p} \frac{a^2}{12(a + e)^2} \left(\frac{\pi}{s_e}\right)^2 \left[\left(\frac{e}{a}\right)^3 + \left(\frac{e - b}{a + b} + \frac{b}{a}\right)^2\right] \tag{4.184}$$

where I_p = moment of inertia, in per in, of plate alone = $t_p^3/10.92$
s_e = effective rib span for torsion, in = $0.81s$
s = rib span, in

As for open ribs, analysis of an orthotropic plate with closed ribs is facilitated by use of influence coefficients. For computation of these coefficients, Eq. (4.178) reduces to the homogeneous equation

$$D_y \frac{\partial^4 w}{\partial y^4} + 2H \frac{\partial w^4}{\partial x^2 \, \partial y^2} = 0 \tag{4.185}$$

The solution can be given as an infinite series consisting of terms of the form

$$w_n = (C_{1n} \sinh \alpha_n y + C_{2n} \cosh \alpha_n y + C_{3n} \alpha_n y + C_{4n}) \sin \frac{n\pi x}{l} \tag{4.186}$$

where n = integer ranging from 1 to ∞ (odd numbers for symmetrical loads)
l = floorbeam span, in
x = distance, in, from girder
C_m = integration constant, determined by boundary conditions

$$\alpha_n = \frac{n\pi}{l} \sqrt{\frac{2H}{D_y}} \tag{4.187}$$

$\sqrt{H/D_y}$ is called the **plate parameter**.

Because of the sinusoidal form of the deflection surface [Eq. (4.186)] in the x direction, it is convenient to represent loading by an equivalent expressed in a Fourier series [Eqs. (4.169) to (4.174)]. Convergence of the series may be improved, however, by distributing the loading over a width smaller than l but larger than that of the actual loading.

Influence coefficients for the ribs may be computed with the use of a carry-over factor κ_n for a sinusoidal moment applied at a rigid support. If a moment M is applied at one support of a continuous closed rib, the moment induced at the other end is κM. The carry-over factor for a closed rib is given by

$$\kappa_n = \sqrt{k_n^2 - 1} - k_n \tag{4.188}$$

where $k_n = (\alpha_n s \coth \alpha_n s - 1)/\beta_n$
$\beta_n = 1 - \alpha_n s/\sinh \alpha_n s$

Thus there is a carry-over factor for each value of n.

Next needed for the computation of influence coefficients are shears, reactions, support moments, and interior moments in a rib span as a sinusoidal load with unit amplitude moves

over that span. Since an influence curve also is a deflection curve for the member, these values can be obtained from Eq. (4.186). Consider a longitudinal section through the deflection surface at $x = l/2n$.

Then the influence coefficient for the moment at the support from which y is measured may be computed from

$$m_{0n} = \frac{\kappa_n s}{\beta_n(1 - \kappa_n^2)} \left[-\frac{\kappa_n - \cosh \alpha_n s}{\sinh \alpha_n s} \sinh \alpha_n y - \cosh \alpha_n y + (\kappa_n - 1)\frac{y}{s} + 1 \right] \tag{4.189}$$

The coefficient should be determined for each value of n. (If the loading is symmetrical, only odd values of n are needed.) To obtain the influence coefficient when the load is in the next span, m_{0n} should be multiplied by κ_n. And when the load is in either of the following two spans, m_{0n} should be multiplied by κ_n^2 and κ_n^3, respectively.

The influence coefficient for the bending moment at midspan may be calculated from

$$m_{Cn} = \frac{\sinh \alpha_n y}{2\alpha_n \cosh (\alpha_n s/2)} + \frac{\kappa_n s}{2\beta(1 - \kappa_n) \cosh (\alpha_n s/2)} \times \left(\tanh \frac{\alpha_n s}{2} \sinh \alpha_n y - \cosh \alpha_n y + 1 \right) \quad y \le \frac{s}{2} \tag{4.190}$$

With the influence coefficients known, the bending moment in the rib at $x = l/2n$ can be obtained from

$$M_0 = (a + e) \sum_{n=1}^{\infty} Q_{nx} m_{0n} \qquad \text{or} \qquad M_C = (a + e) \sum_{n=1}^{\infty} Q_{nx} m_{Cn} \tag{4.191}$$

for each equivalent load Q_{nx}. As before, a is the width (in) of the rib at the plate and e is the distance (in) between adjoining ribs (Fig. 4.36).

Closed-Rib Deck-Member III, First Stage. In this stage, the rib reactions on the floorbeams are computed on the assumption that the beams provide rigid support. The reactions may be calculated with the influence coefficients in Table 4.5. The effective width of plate acting as top flange of the floorbeam may be obtained from Table 4.7 with s_f equal to the floorbeam spacing and, for a simply supported beam, $l_e = l$.

Closed-Rib Deck-Members II and III, Second Stage. The analysis for the case of floorbeams providing elastic support is much the same for a closed-rib deck as for open ribs. Table 4.8 can supply the needed influence coefficients. The flexibility coefficient, however, should be computed from

$$\gamma = \frac{l^4 I_r}{\pi^4 s^3 (a + e) I_f} \tag{4.192}$$

Similarly, the change in midspan moment in a rib can be found from Eq. (4.176) with $a + e$ substituted for a. And the change in floorbeam moment can be obtained from Eq. (4.177). The effective width of plate used for first-stage calculations generally can be used for the second stage with small error.

Closed-Rib Deck-Member IV. The girders are analyzed by conventional methods. The effective width of plate as the top flange on one side of each girder may be taken as half the distance between girders on that side.

(*Design Manual for Orthotropic Steel Plate Deck Bridges,* American Institute of Steel Construction, Chicago, Ill.; M. S. Troitsky, *Orthotropie Bridges Theory and Design,* The James F Lincoln Arc Welding Foundation, P.O. Box 3035, Cleveland, Ohio 44117; 5. P. Timoshenko and S. Woinowsky-Krieger, *Theory of Plates and Shells,* McGraw-Hill, Inc., New York.)